NOAA Technical Memorandum ERL GLERL-72

CURRENTS, TEMPERATURES, AND DIVERGENCES OBSERVED IN EASTERN CENTRAL LAKE MICHIGAN DURING MAY-OCTOBER 1984

Erik S. Gottlieb
James H. Saylor
Gerald S. Miller

Great Lakes Environmental Research Laboratory
Ann Arbor, Michigan
October 1989

UNITED STATES
DEPARTMENT OF COMMERCE

Robert A. Mosbacher
Secretary

NATIONAL OCEANIC AND
ATMOSPHERIC ADMINISTRATION

John A. Knauss
Under Secretary for Oceans
and Atmosphere/Administrator

Environmental Research
Laboratories

Joseph 0. Fletcher
Director

NOTICE

Mention of a commercial company or product does not constitute an endorsement by NOAA Environmental Research Laboratories. Use for publicity or advertising purposes of information from this publication concerning proprietary products or the tests of such products is not authorized.

For sale by the National Technical Information Service, 5285 Port Royal Road
Springfield, VA 22161

CONTENTS

FIGURES

TABLES

CURRENTS, TEMPERATURES, AND DIVERGENCES OBSERVED IN EASTERN CENTRAL LAKE MICHIGAN DURING MAY-OCTOBER 1984

Erik S. Gottlieb, James H. Saylor, and Gerald S. Miller

ABSTRACT. An array of four instrumented moorings covering an area of 150 km^2 was in place approximately 40 km offshore in eastern central Lake Michigan during May-October 1984. Each mooring supported current meters at the depth levels 5, 10, 20, 30, 50, and 100 m, and a thermistor chain between 6 and 46 m depth. The current velocity data were used to compute the divergence and curl across the array area at each depth level. Two or three events of large southeastward currents, north-south alternating wind bursts, upwelled thermocline, and increased positive divergence and negative curl were observed from mid-August to early September.

1. INTRODUCTION

During May-October 1984 a triangular-shaped array of four pairs of instrumented moorings collected data approximately 40 km offshore in eastern central Lake Michigan (Figure 1). The mooring pairs were spaced 10 and 17 km apart, and each pair supported EG&G vector-averaging current meters (VACMs) at 5, 10, 20, 30, and 50 m depth and at 1 m above the bottom, and a thermistor chain between 6 and 46 m depth (Figure 2). The primary moorings (1, 2, 3, and 4) supported the VACMs at 10, 20, 30, and 50 m depth, and the secondary moorings (1A, 2A, 3A, and 4A) supported the VACMs at 5 m depth and 1 m above the bottom, and the thermistor chains. The position, water depth, and deployment and recovery times for each mooring pair are listed in Table 1. Data from the VACMs on mooring 4 at 3, 5, 7, and 9 m above the bottom were used to study the velocity structure within the bottom Ekman layer (Saylor and Miller, 1986, 1988). Readers interested in bottom boundary layer phenomena are directed to the 1988 paper.

This report contains plots of the current velocities (Figure 3 and Appendix A), water temperatures (Appendices B and C), divergence and curl computed across the array area at each depth level (Appendices C and D), and meteorological data (Figure 4) from the National Data Buoy Center (NDBC) buoy 45007 in south central Lake Michigan (see Figure 1 for location). These data show the spatial (both horizontal and vertical) and temporal variability of the currents and thermal structure in Lake Michigan during spring and summer.

2. DATA DESCRIPTION

The water depth and starting and stopping times of the data collection period are listed for each instrument in Table 2. All moorings except 1 and 1A were deployed at their intended water depths, so the reference and actual depths are equal (for the VACMs at 1 m above the bottom, the reference depth is 100 m). All instruments yielded full data returns except VACM 556 (mooring 3, 50 m), which malfunctioned from deployment until July 13, and VACM 571 (mooring 3A, 100 m), which malfunctioned during the periods July 15-16 and August l-8.

[1]GLERL Contribution No. 679

The velocity and temperature data were recorded by the VACMs at 15-minute intervals, and later averaged at hourly intervals. The thermistor data were recorded at hourly intervals. The meteorological data (barometric pressure, air temperature, and wind stress computed from velocity at 5 m above the lake surface) were measured from the NDBC buoy at hourly intervals. All aformentioned hourly data are herein referred to as "raw" data. A Cosine-Lanczos filter with a 60-point taper (40-hour half-power point), described by Mooers and Smith (1968), was applied to all raw data. Unless otherwise noted, all computations and data presentations described here use the filtered data.

3. COMPUTATIONS

To examine the variability of the currents and temperatures, and to provide evidence of upwelling and downwelling events, the divergence $\nabla \cdot \mathbf{V}$ and curl $\nabla \times \mathbf{V}$ of the horizontal current velocity field V = ux + vy (where boldface denotes vector quantities, u and v are the measured velocity components, and x and y are unit vectors in the east and north directions) were computed across the array area at each depth level (Appendix C). The water temperatures are also plotted in Appendix C for comparison with the divergences (positive divergence in the surface layer indicates upwelling, negative divergence indicates downwelling). To examine the spatial scale of the variability, the divergence was also computed separately (Appendix D) across each of the three small triangles (see Figure 1) of the array area.

The wind stress (Figure 4) was computed using $\tau = C_d W^2$, where W is the measured wind speed and Cd(W) is the drag coefficient computed using the method of Liu and Schwab (1987). Under the assumption of no air-sea temperature difference (i.e., neutral stability), Cd becomes an almost linear function of W. For the data in Figure 4, the minimum, maximum, mean, and standard deviation values of Cd are 0.00012, 0.00215, 0.00102, and 0.00026.

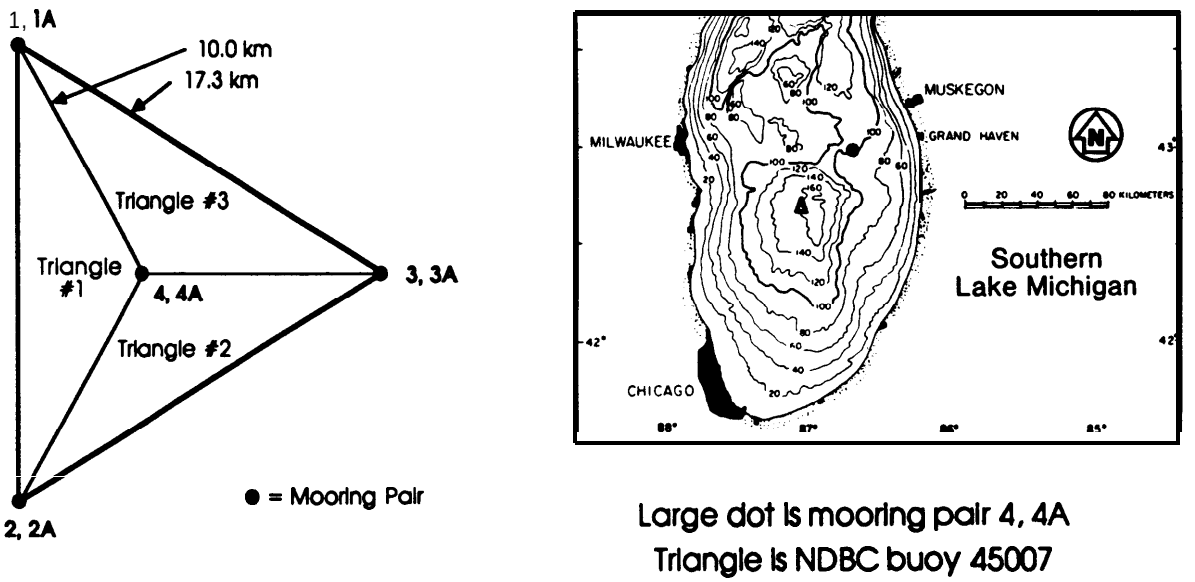

Figure 1.--Location and schematic diagram of the array of instrumented moorings. The curl and divergence (Appendix C) are computed across the big triangle (123), and the separated divergences (Appendix D) are computed across the smaller, labeled triangles (124,234 and 134).

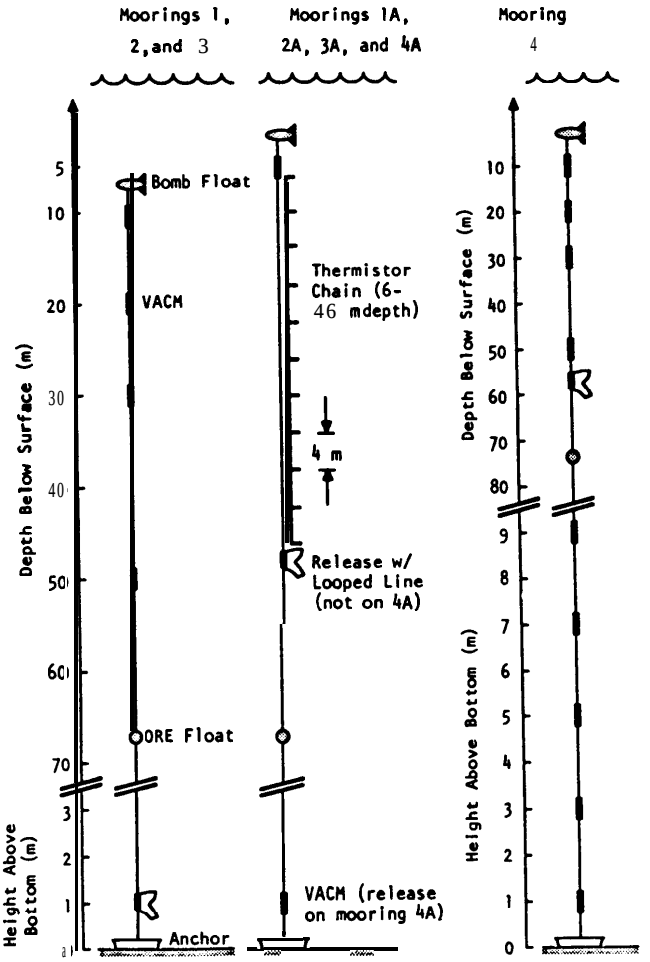

Figure 2.--Schematic diagrams of the moorings indicating current meter (VACM) and thermistor depths. Data from the five near-bottom current meters on mooring 4 were described by Saylor and Miller (1988).

4. DATA PRESENTATIONS

At the two offshore locations (moorings 1 and 2), the monthly-averaged current velocities (Figure 3) were very small from May to August. Inshore (moorings 3 and 4), the currents were also very small in June and July, although the northeastward surface layer drift (above 20-30 m depth) in July appears well correlated with the weaker surface flow offshore. During August a strong south-southeastward surface current and a weaker east-southeastward current developed at the most shoreward and center moorings (3 and 4), respectively. Comparing the bidaily-averaged currents (Appendix A) and the wind stress (Figure 4) shows that the strong southeastward surface currents characterized the lake's response to the north-south-alternating, 2-day-long wind bursts that occurred after mid-August. The wind was steady and southerly during the last week in August, but abruptly changed to a pattern of mostly north-south-alternating, 2- to 4-day-long intense wind stress impulses that continued throughout much of September.

During September, the monthly-averaged inshore currents (Figure 3) were southward throughout the surface layer, while the offshore currents were strongly sheared throughout the entire water column (i.e., southwestward flow at mooring 2 and mostly northeastward flow at mooring 1). The divergent surface flow (i.e., volume outflow from the surface layer) suggested from this pattern was confirmed by computation at each depth level (Appendix C). During the last week in August the computed divergence became increasingly large and positive (i.e., volume outflow), especially in the surface layer, and remained so throughout most of September.

Table 1 .-Location, water depth, deployment and recovery times, and distance separating the moorings for each mooring pair

Mooring	Latitude (deg min sec)	Longitude (deg min sec)	Water Depth (m)	Deployment Date	Deployment Time (EST)	Recovery Date	Recovery Time (EST)	Distance Between Moorings (m)
	43' 05' 44.0"	86' 42' 47.4"	107	May 10	0945	Oct.16	1415	275
1A	43' 05' 39.4"	86' 42' 36.6"	108	May 10	1040	Oct. 16	1343	275
2	42' 56' 07.4"	86' 42' 35.1 .	97.3	June 6	1025	Oct. 16	1015	110
2A	42' 56' 09.9"	86' 42' 33.7	97.3	June 6	1120	Oct. 16	1210	110
3	43' 00' 54.0"	86' 31' 28.7	91	May 7	0920	Oct. 15	1250	430
3A	43' 01' 08.2"	86' 31' 37.8"	91	May 7	1110	Oct. 15	1200	430
4	43' 00' 52.1"	86' 39' 00.0"	102	June 6	1755	Oct. 15	1015	88
4A	43' 00' 55.1"	86' 38' 58.8"	102	June 6	1840	Oct. 15	1100	88

Table 2.-Instrument depth, and starting and stopping times of usable data for each current meter (VACM) and thermistor chain (THERM)

Instrument Type and #	Mooring	Reference/ Actual Depth* (m)	Start Point Date	Start Point Time (EST)	Stop Point Date	Stop Point Time (EST)
VACM 347	1A	5 / 8	May 10	1200	Oct. 16	1300
VACM 572	1	10 / 6.3	May 10	1300	Oct. 16	1300
VACM 279	1	20 / 16.3	May 18	1700	Oct. 16	1300
VACM 352	1	30 / 26.3	May 10	1200	Oct. 16	1300
VACM 552	1	50 / 46.3	May 10	1200	Oct. 16	1300
VACM 575	1A	100 / 107	May 10	1200	Oct. 16	1300
VACM 353	2A	5 / —	June 6	1400	Oct. 16	1100
VACM 584	2	10 / —	June 6	1300	Oct. 16	0900
VACM 275	2	20 / —	June 6	1300	Oct. 16	0900
VACM 280	2	30 / —	June 6	1300	Oct. 16	0900
VACM 570	2	/ —		1300	Oct. 16	0900
		/		1400	Oct. 16	1100
		5 / —	May 7	1300	Oct. 15	1200
VACM 567	3	10 / —	May 7	1200	Oct. 15	1200
VACM 315	3	/ —	May 7	1100	Oct. 15	1200
VACM 311	3	30 / —	May 7	1100	Oct. 15	1200
VACM 556	3	50 / —	July 13	0200	Oct. 15	1200
VACM 571	3A	100 / 90	May 7	1300	Oct. 15	1200
VACM 555	4A	5 / —	June 6	2100	Oct. 15	1000
VACM 550	4	10 / —	June 6	2100	Oct. 15	0900
VACM 274	4	20 / —	June 6	2000	Oct. 15	0900
VACM 349	4	30 / —	June 6	2000	Oct. 15	0900
VACM 569	4	50 / —	June 6	2000	Oct. 15	0900
VACM 574	4A	100 / 101	June 6	2000	Oct. 15	0900
THERM 316	1A	6-46 / 9-49	May 10	1200	Oct. 16	1300
THERM 313	2A	6-46 / —	June 6	1400	Oct. 16	1100
THREM 315	3A	6-46 / —	May 7	1300	Oct. 15	1200
THERM 305	4A	6-46 / —	June 6	2100	Oct. 15	1000

. The reference (intended) depths are the VACM depth levels (5, 10, 20, 30, 50, and 100 m) referred to throughout this report (the VACMs at 100 m reference depth were actually 1 m above the bottom). The reference and actual depths of the instruments on moorings 1 and 1A differ because of fathometer error during the mooring deployment.

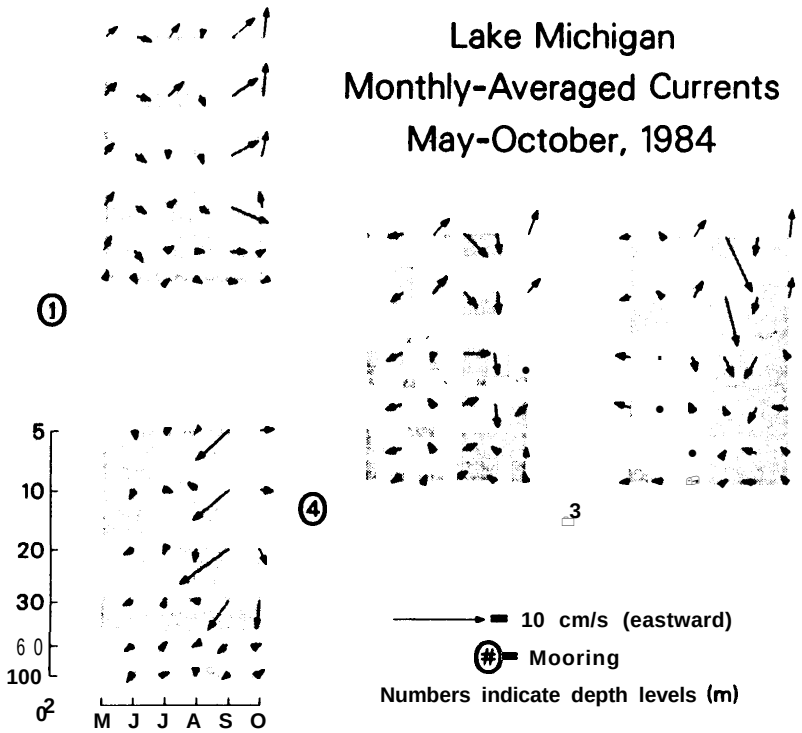

Figure 3.--Monthly-averaged currents computed from the raw data at each depth level for each mooring. The sticks point toward the direction the current is heading (north is up).

From mid-August until September 7, the thermocline (Appendices B and C) was determined to be steadily upwelling (most notable inshore at the 20 and 30 m depth levels), but thereafter abruptly downwelled to its normal, late-summertime depth level (about 24-28 m). The upwelling thermocline correlated well with the divergent surface flow during the same period. The divergent surface flow would have caused a lowering of the still-water level by about 1 m if it had not been balanced by convergence (volume inflow) at some deeper level. Interestingly, convergence was not observed at the 50 or 100 m depth levels (Figs. C.5 and C.6). Also, the divergence occurred mainly across the offshore triangle of moorings (triangle 1, Appendix D).

Sample plots of the raw velocity and temperature data during August and September from 20 m depth at moorings 1 and 3 (Appendix E) reveal intense and omnipresent near-inertial-period oscillations (of about 18-hour period) of the thermocline surface. It is believed that the modulation of the inertial oscillation envelope is due to the concurrent propagation of basin-scale internal waves of near-inertial periodicity (Mortimer, 1971). The observed thermocline oscillations were used in a study of primary production variations caused by thermocline depth fluctations (Fahnenstiel, et al., 1988).

5. REFERENCES

FAHNENSTIEL, G.L., D. SCAVIA, G.A. LANG, J.H. SAYLOR, G.S. MILLER, and D.J. SCHWAB. Impact of inertial period internal waves on fixed-depth primary production estimates. Journal of Plankton Research 10(1):77-87 (1988).

LIU, P.C., and D.J. SCHWAB. A comparison of methods for estimating u_* from given u_z and air-sea temperature differences. Journal of Geophysical Research 92(C6):6488-6494 (1987).

Mooers, C.N.K., and R.L. Smith. Continental shelf waves off Oregon. Journal of Geophysical Research 73(2):549-557 (1968).

Mortimer, C.H. Large-scale oscillatory motions and seasonal temperature changes in Lake Michigan and Lake Ontario. Special Report No. 12, Center for Great Lake Studies, Univ. of Wisconsin, Milwaukee, WI, 217 pp. (1971).

SAYLOR, J.H., and G.S. MILLER. Lakes environment benthic boundary layer experiments: Detailed Technical Plan for the Great Lakes Environmental Research Laboratory, January 1986, Ann Arbor, MI, 300 pp. (1986).

SAYLOR, J.H., and G.S. MILLER. Observations of Ekman veering at the bottom of Lake Michigan. Journal of Great Lakes Research 14(1):94-100 (1988).

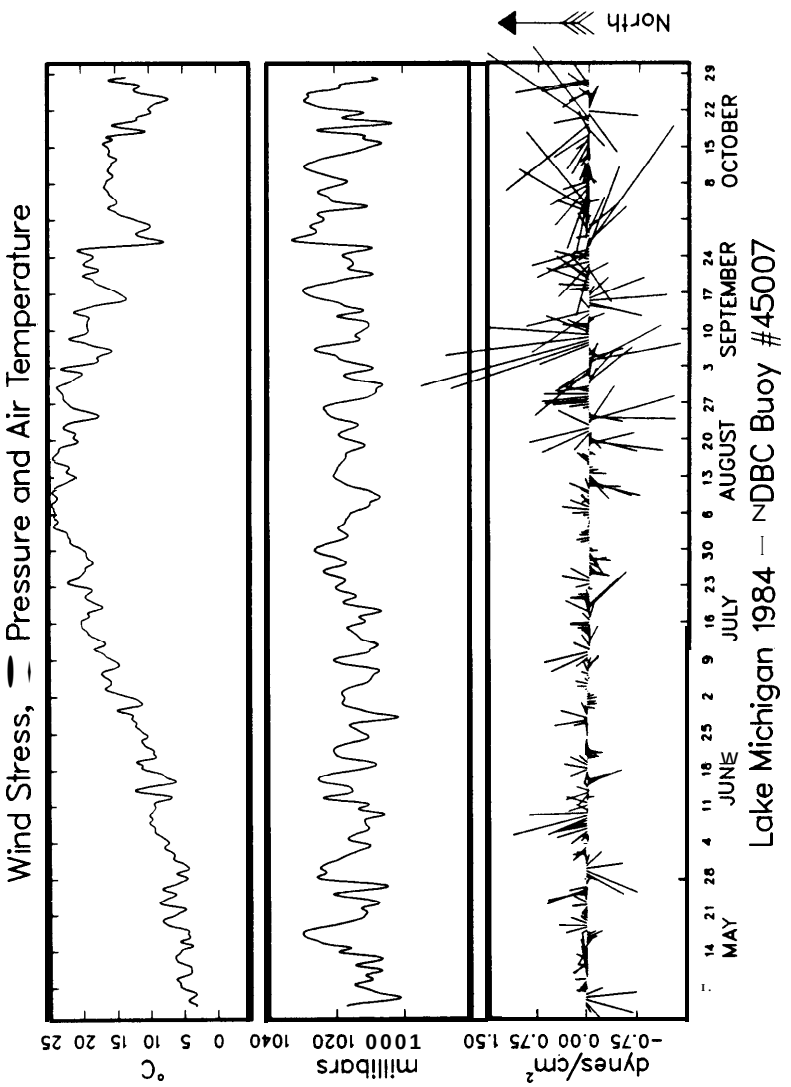

Figure 4.--Low-pass filtered, bidaily-averaged wind stress (bottom panel, the sticks point toward the direction the wind is heading), barometric pressure (middle panel), and air temperature (top panel) at 5 m above the water surface in south central Lake Michigan (see Figure 1 for location).

Appendix A: Bidaily-Averaged Currents

Stick diagrams of low-pass-filtered, bidaily-averaged currents for each mooring, at the following depths:

Figure A.1--5 m
Figure A.2--10 m
Figure A.3--20 m
Figure A.4--30 m
Figure AS-50 m
Figure A.6--100 m

The sticks point toward the direction the current is heading (north is up).

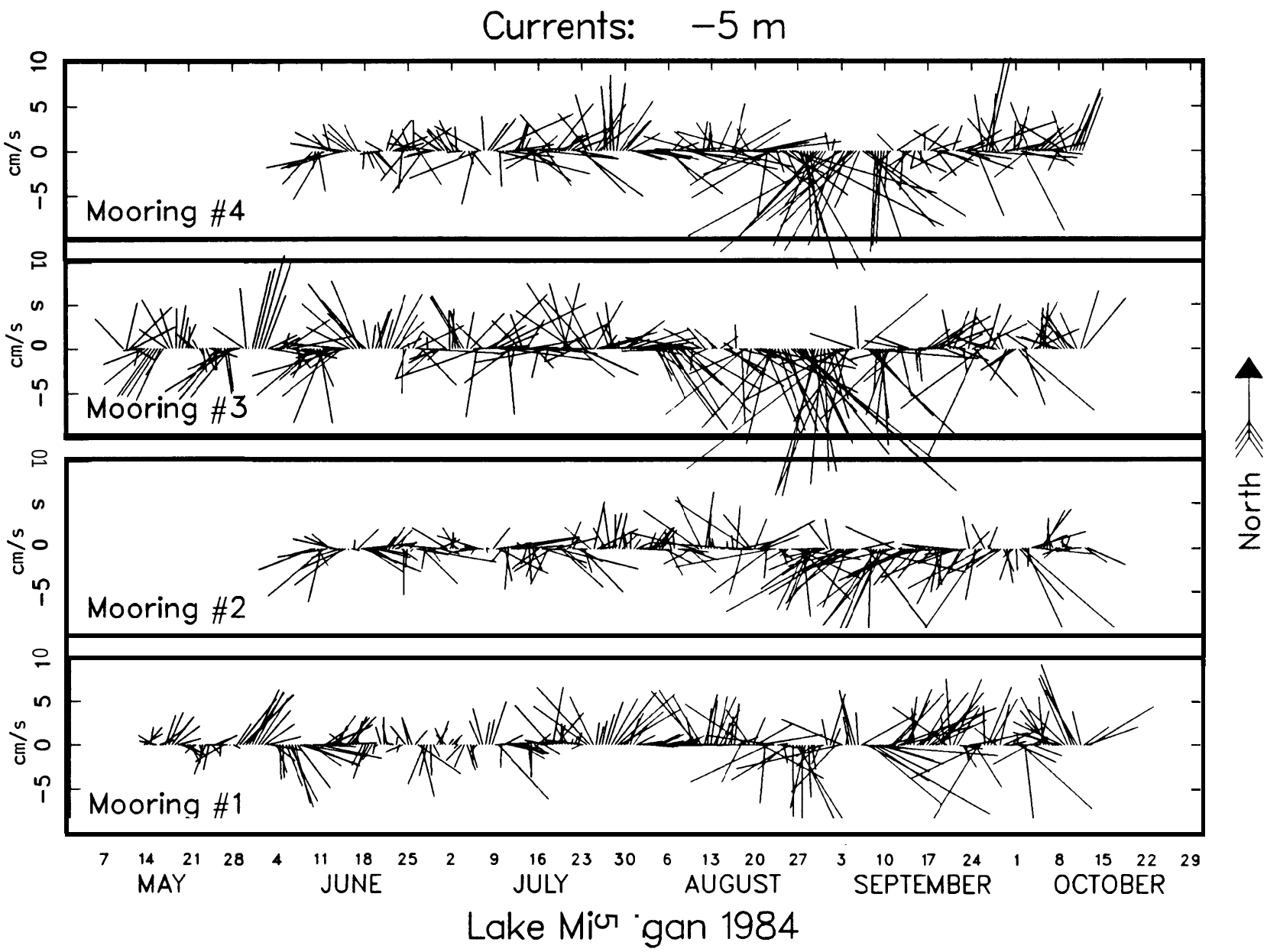
Currents: −5 m
Mooring #4
Mooring #3
Mooring #2
Mooring #1
cm/s
10
5
0
−5
7 14 21 28 4 11 18 25 2 9 16 23 30 6 13 20 27 3 10 17 24 1 8 15 22 29
MAY
JUNE
JULY
AUGUST
SEPTEMBER
OCTOBER
North
Lake Michigan 1984

Figure A 1

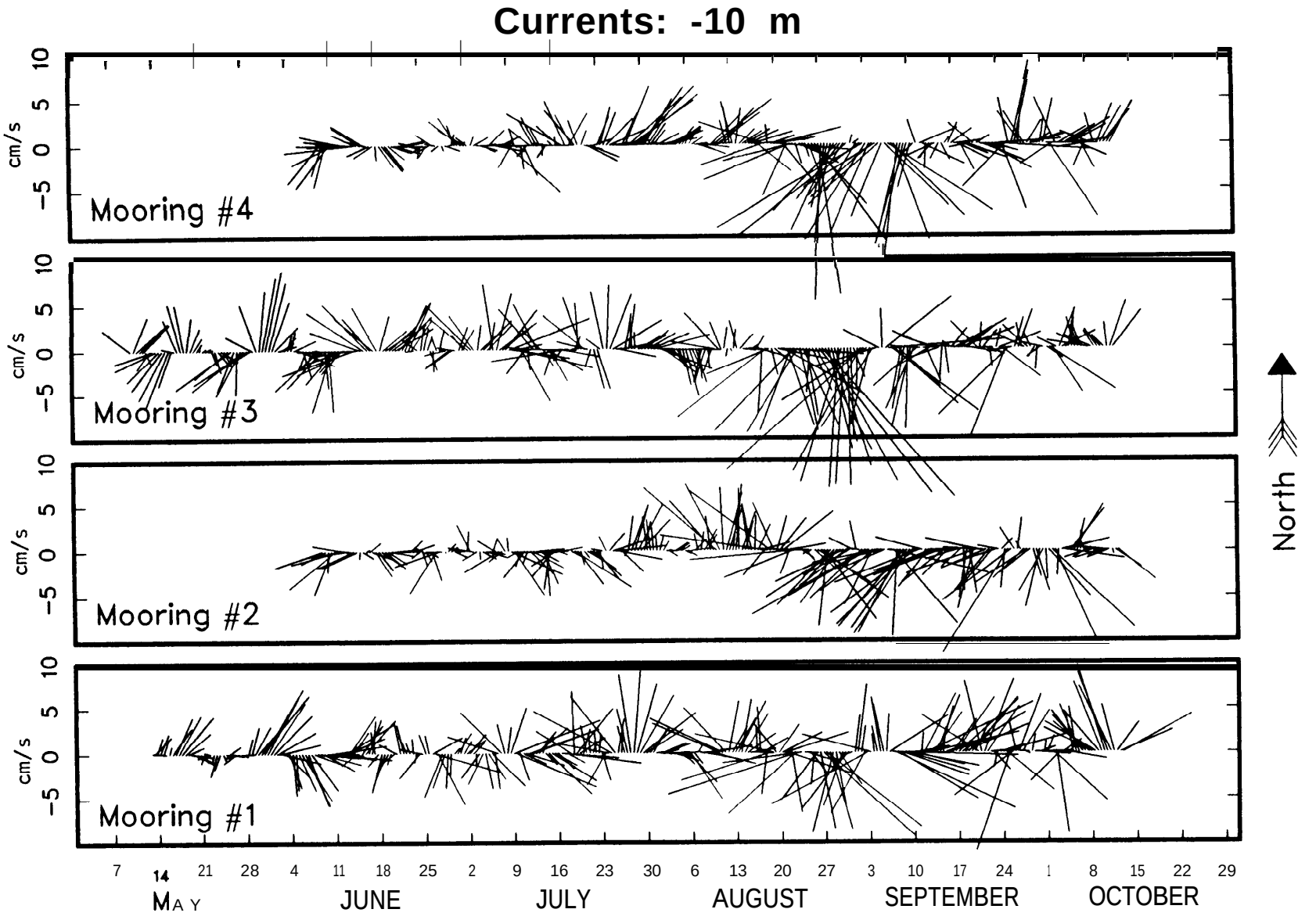

Lake Michigan 1984

Figure A.2

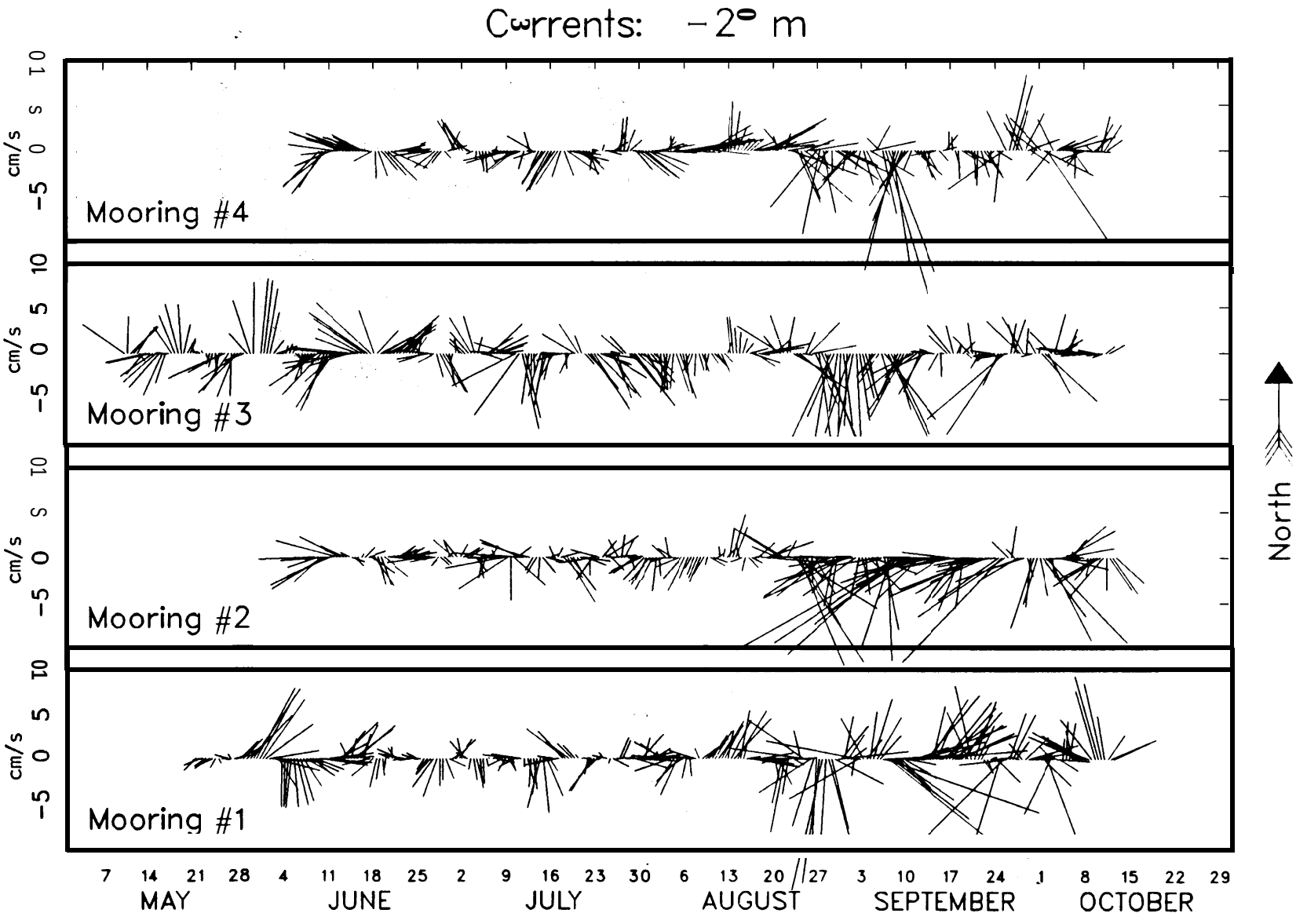

Lake Michigan 1984

Figure A.3

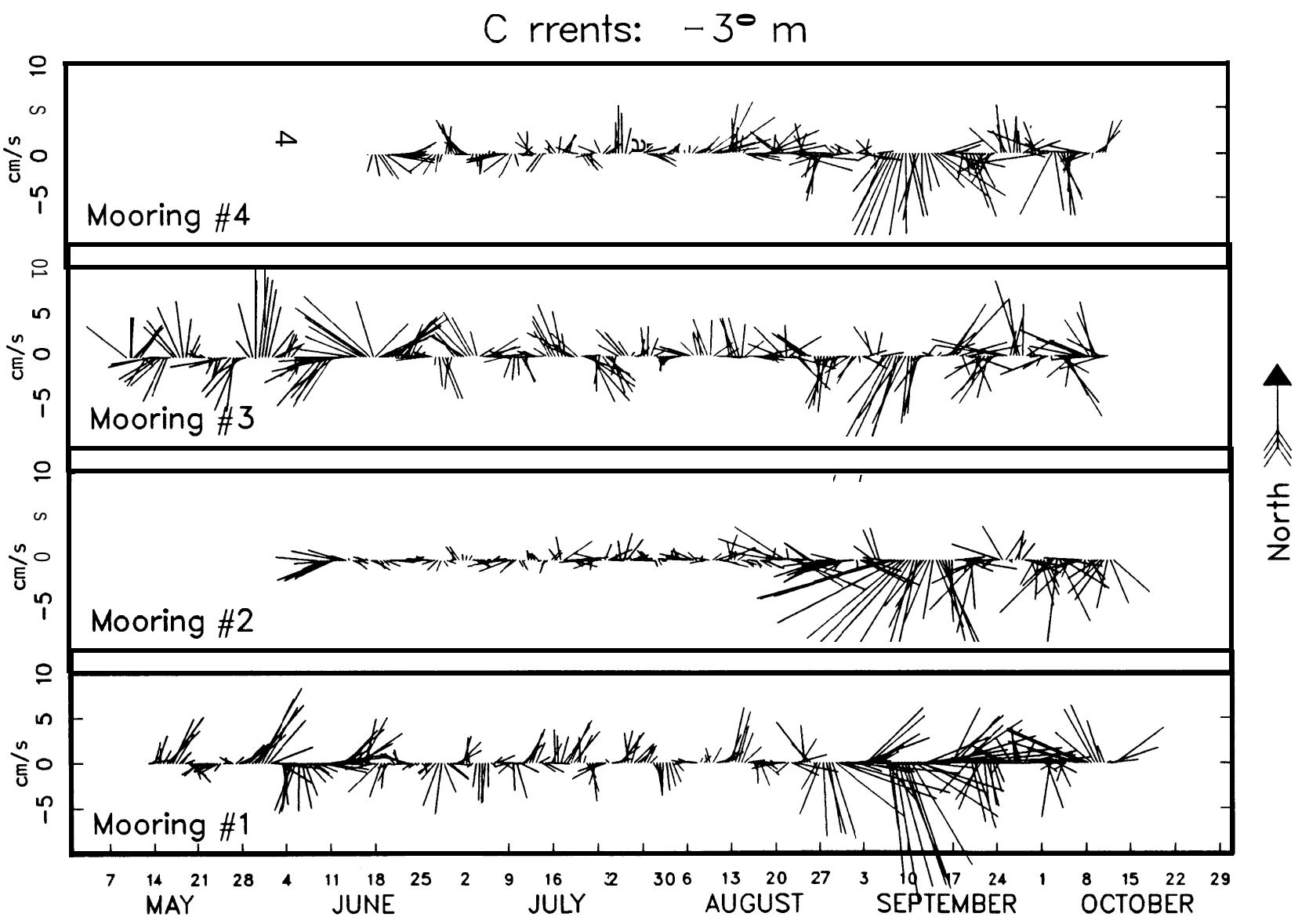
Currents: -3° m
Mooring #4
Mooring #3
Mooring #2
Mooring #1
cm/s
10
5
0
-5
7 14 21 28 4 11 18 25 2 9 16 23 30 6 13 20 27 3 10 17 24 1 8 15 22 29
MAY
JUNE
JULY
AUGUST
SEPTEMBER
OCTOBER
North
Lake Mchigan 1984

Figure A 4

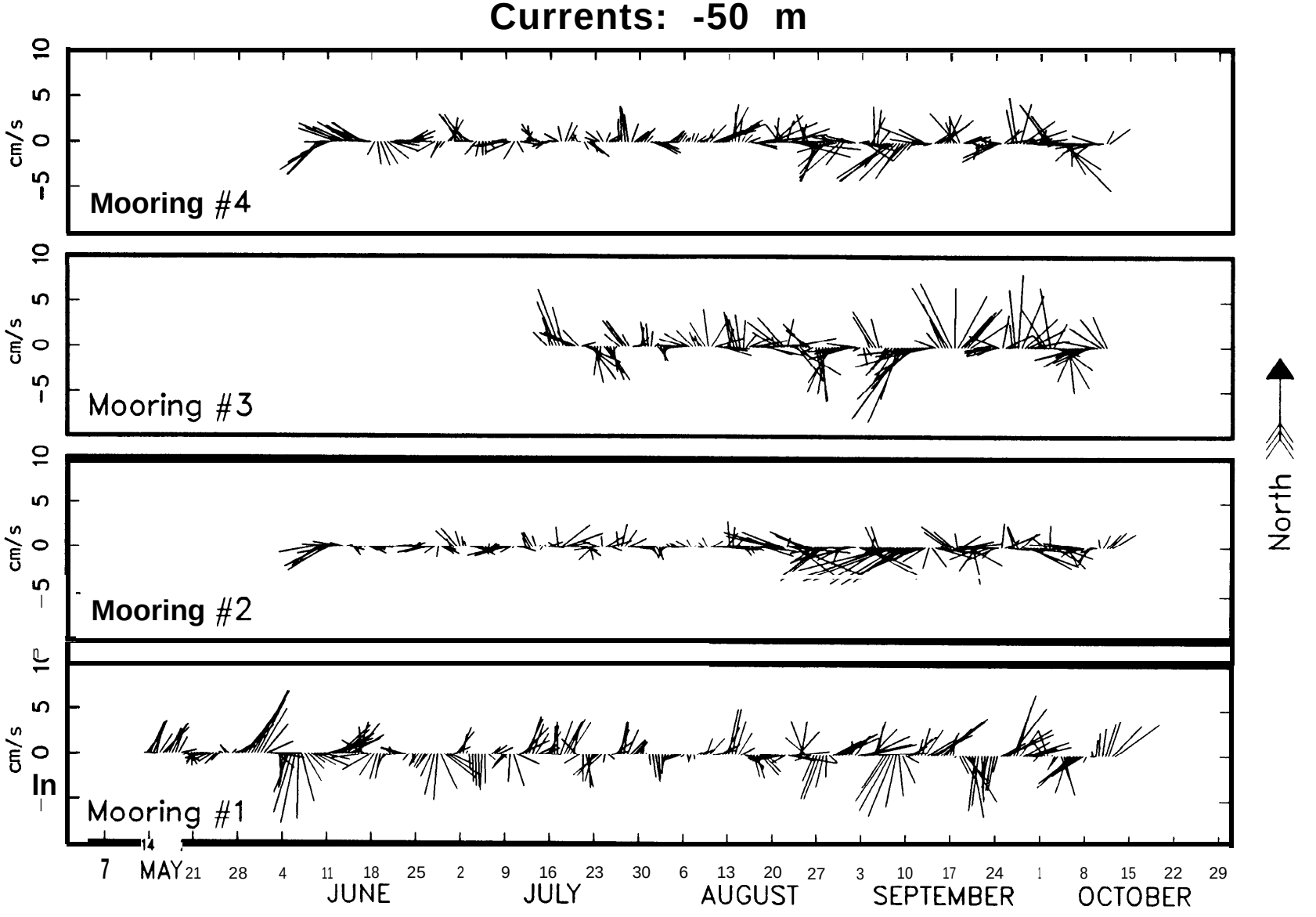

Lake Michigan 1984

Figure A.5

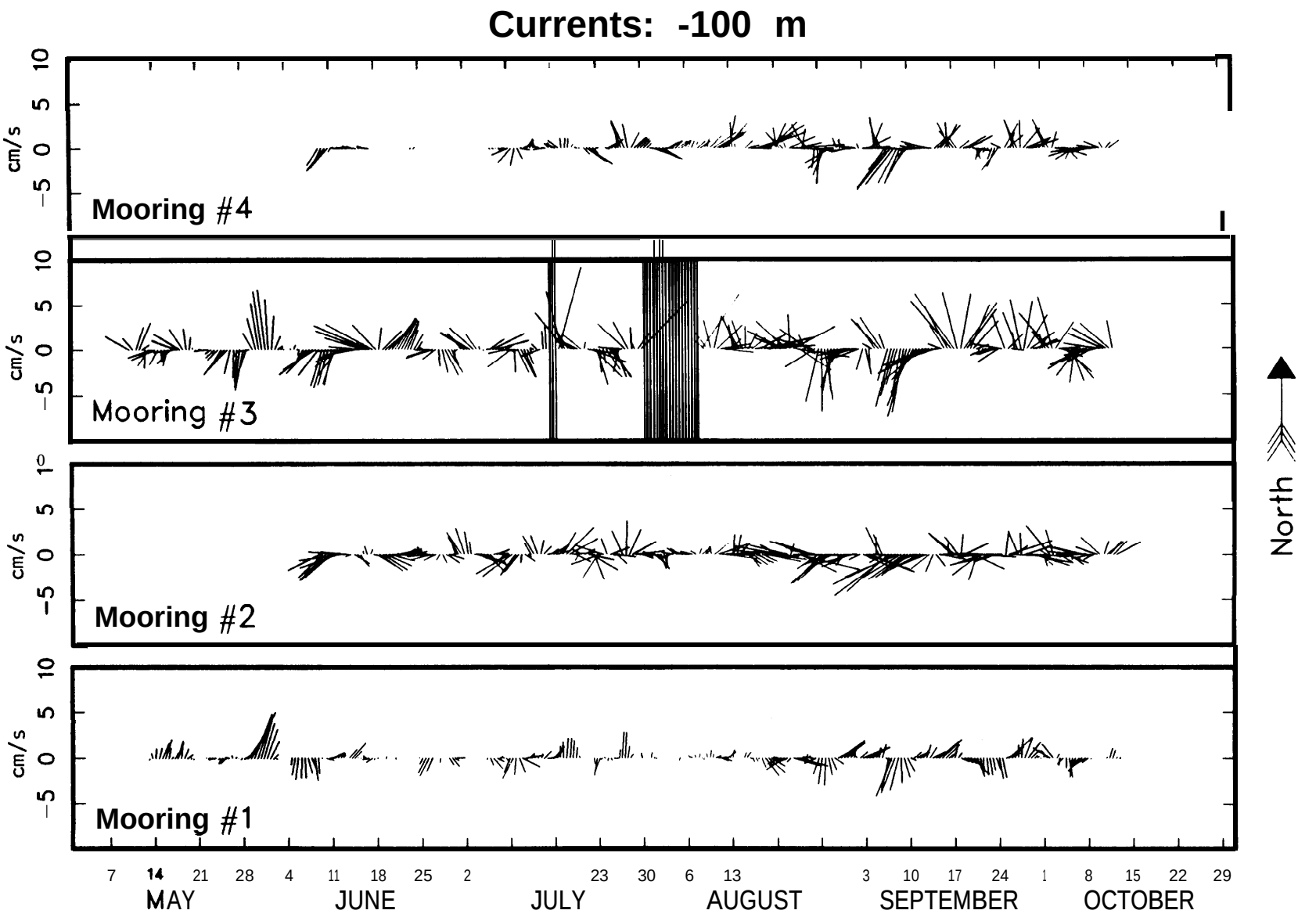

Lake Michigan 1984

Figure A.6

Appendix B: Thermistor Temperatures

Plots of low-pass-filtered thermistor temperatures for the following moorings:

Figure B.1--Mooring 1
Figure B.2--Mooring 2
Figure B.3--Mooring 3
Figure BA-Mooring 4

Thermistors 1-11 were located at the corresponding depths indicated on the left vertical axis. The heavy vertical lines indicate the period of usable data.

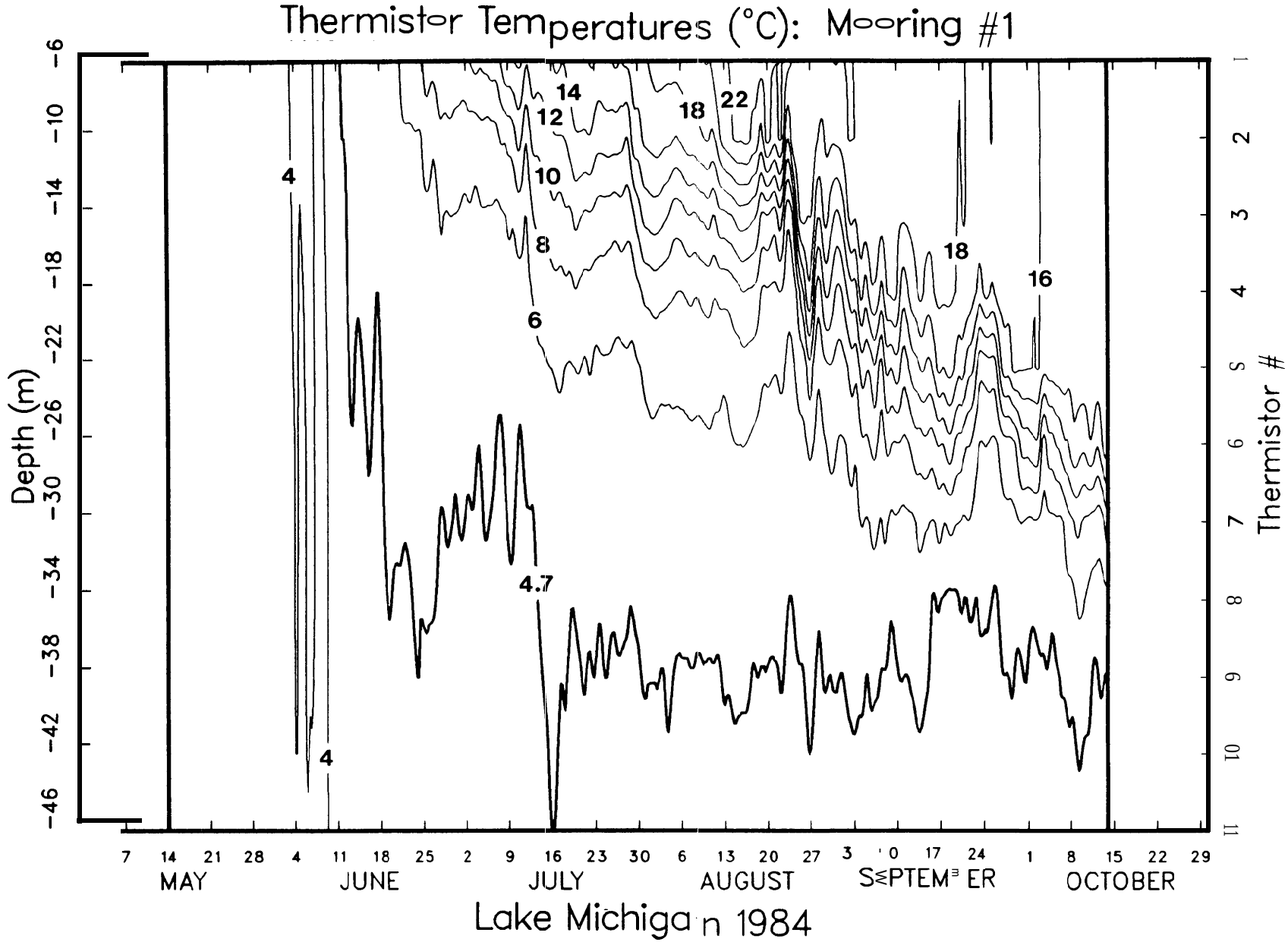
Thermistor Temperatures (°C): Mooring #1
Depth (m)
-6
-10
-14
-18
-22
-26
-30
-34
-38
-42
-46
Thermistor #
1
2
3
4
5
6
7
8
9
10
11
4
4
4.7
6
8
10
12
14
16
18
18
22
7 14 21 28 4 11 18 25 2 9 16 23 30 6 13 20 27 3 10 17 24 1 8 15 22 29
MAY
JUNE
JULY
AUGUST
SEPTEMBER
OCTOBER
Lake Michigan 1984

Figure B. 1

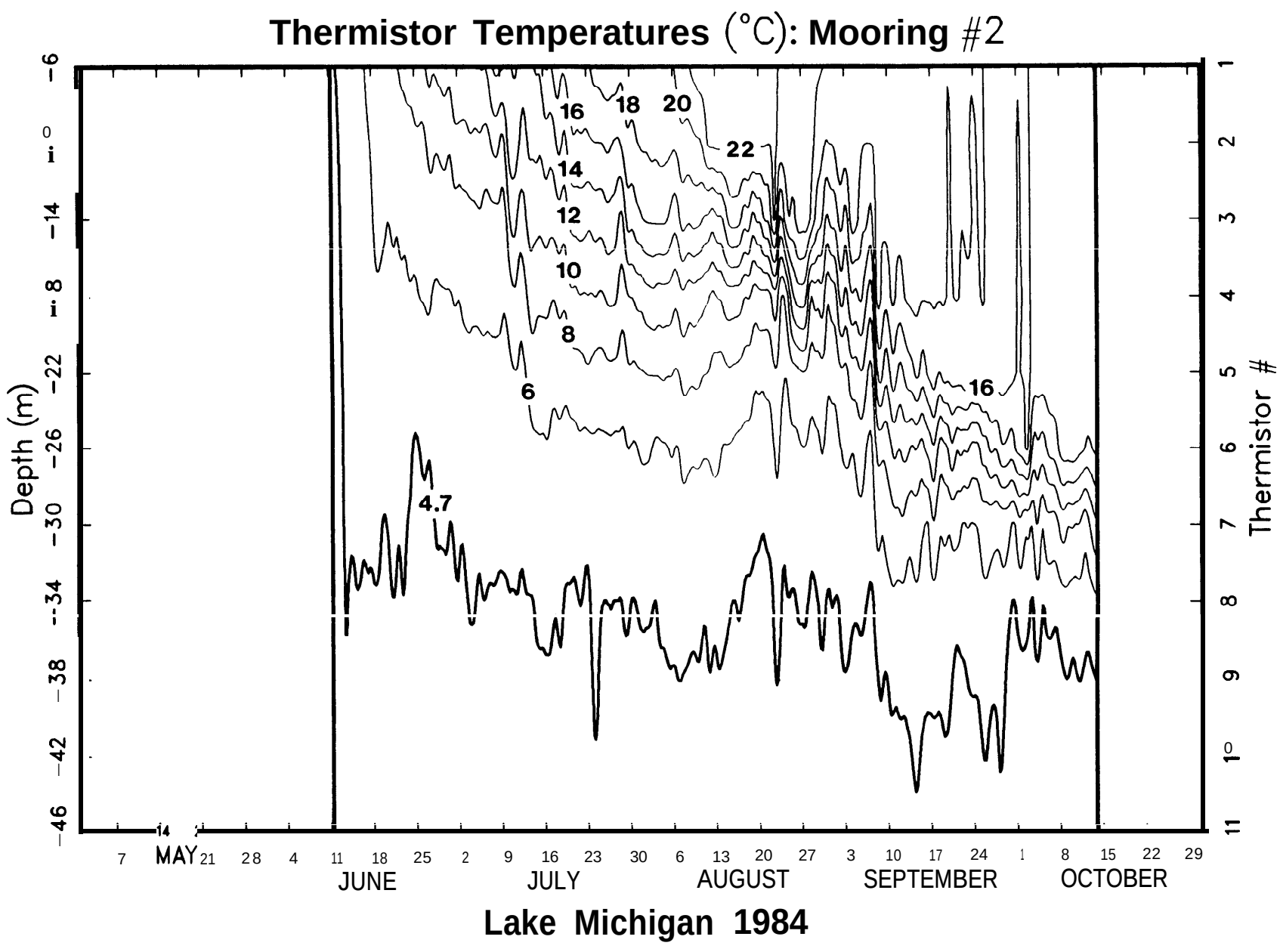
Thermistor Temperatures (°C): Mooring #2
Depth (m)
-6
-14
-22
-30
-38
-46
Thermistor #
1
2
3
4
5
6
7
8
9
10
11
16
18
20
22
14
12
10
8
6
4.7
16
7
MAY
21
28
4
11
18
25
2
9
16
23
30
6
13
20
27
3
10
17
24
1
8
15
22
29
JUNE
JULY
AUGUST
SEPTEMBER
OCTOBER
Lake Michigan 1984

Figure B.2

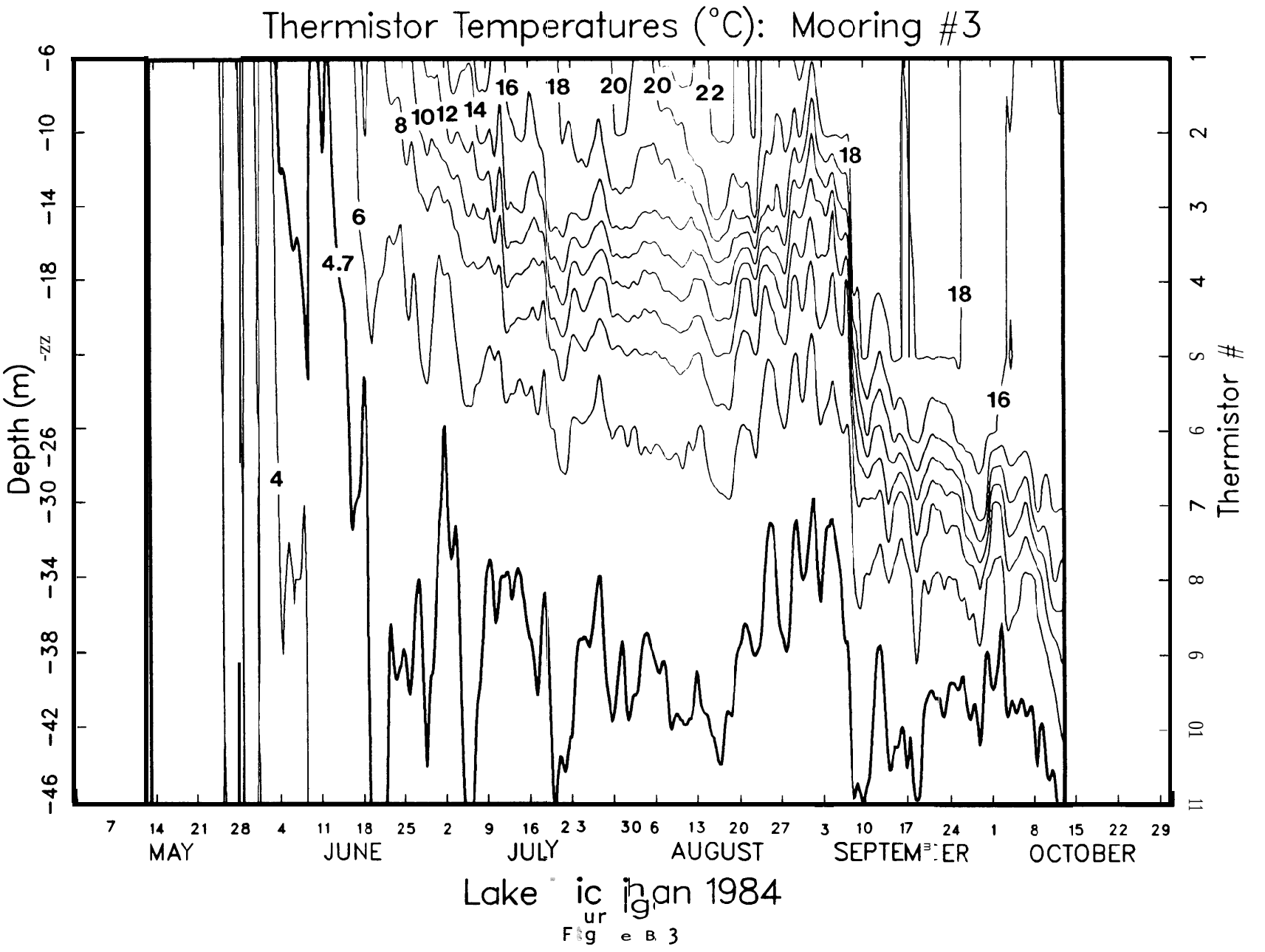

Lake ic ig an 1984

ur

Fg e B. 3

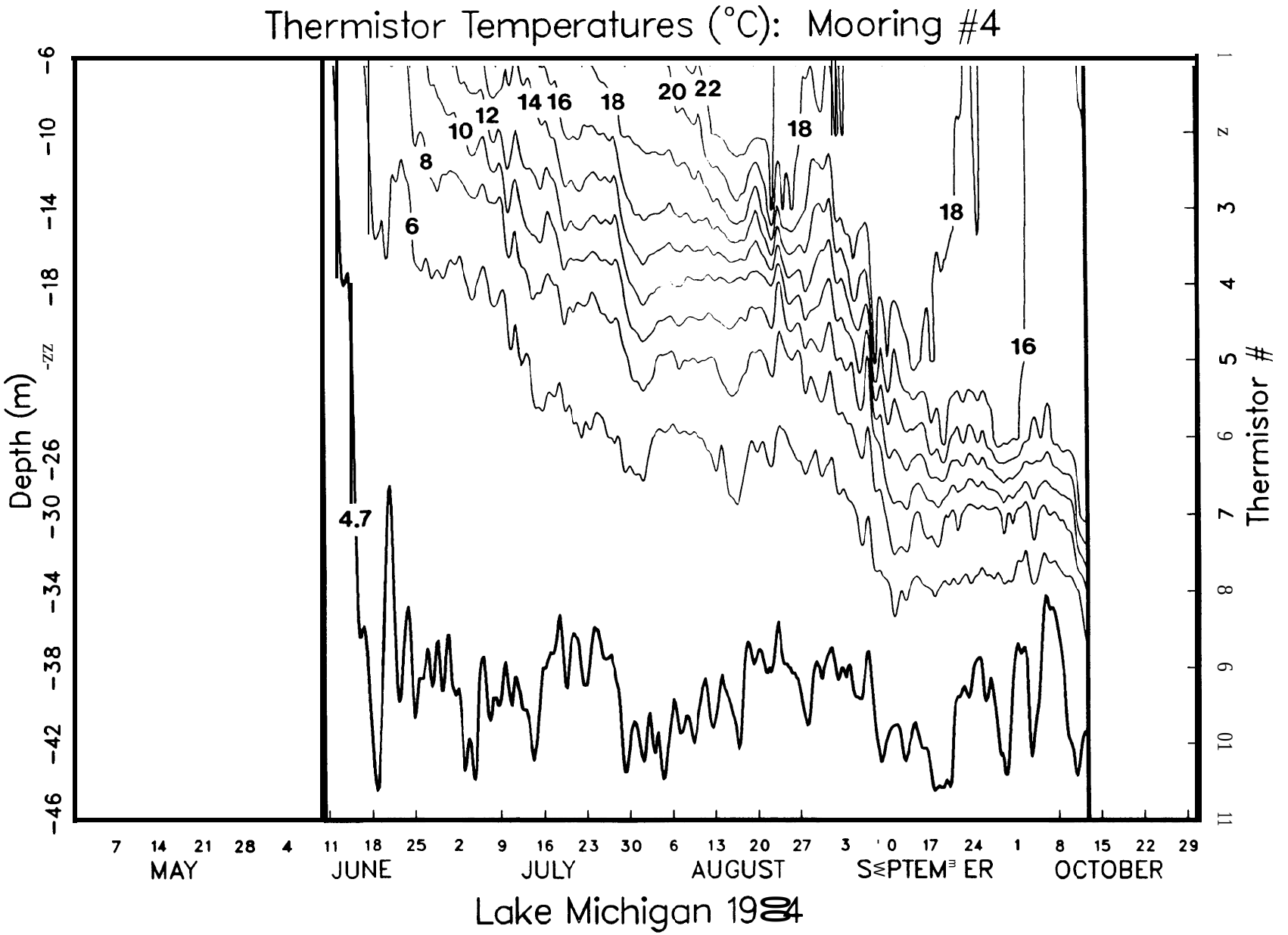
Thermistor Temperatures (°C): Mooring #4
Depth (m)
-6
-10
-14
-18
-22
-26
-30
-34
-38
-42
-46
Thermistor #
1
2
3
4
5
6
7
8
9
10
11
6
8
10
12
14
16
18
20
22
18
18
16
4.7
7 14 21 28 4 11 18 25 2 9 16 23 30 6 13 20 27 3 10 17 24 1 8 15 22 29
MAY
JUNE
JULY
AUGUST
SEPTEMBER
OCTOBER
Lake Michigan 1984

Figure B 4

Appendix C: Temperatures, Divergences, and Curls

Plots of low-pass-filtered temperatures for each mooring (bottom panel), and divergences and curls (top panel) computed across the big triangle (see Figure 1), at the following depths:

Figure C.1--5 m
Figure C.2--10 m
Figure C.3--20 m
Figure C.4--30 m
Figure C.5--50 m
Figure C.6--100 m

For clarity, the temperature curves are offset along the vertical axis by the indicated offset value.

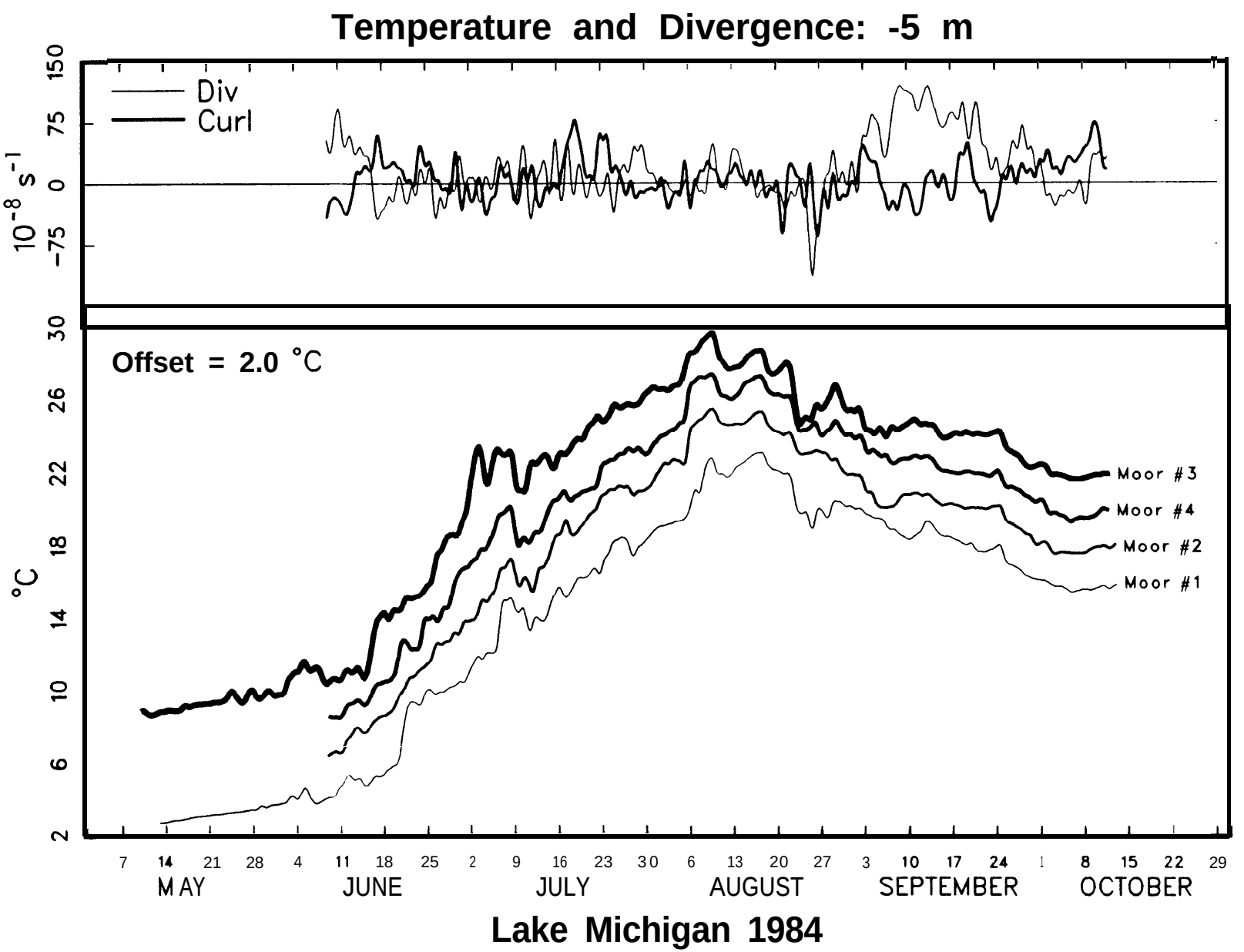
Temperature and Divergence: -5 m
Div
Curl
10^{-8} s^{-1}
150
75
0
−75
Offset = 2.0 °C
°C
30
26
22
18
14
10
6
2
Moor #3
Moor #4
Moor #2
Moor #1
7 14 21 28 4 11 18 25 2 9 16 23 30 6 13 20 27 3 10 17 24 1 8 15 22 29
MAY
JUNE
JULY
AUGUST
SEPTEMBER
OCTOBER
Lake Michigan 1984

Figure C.1

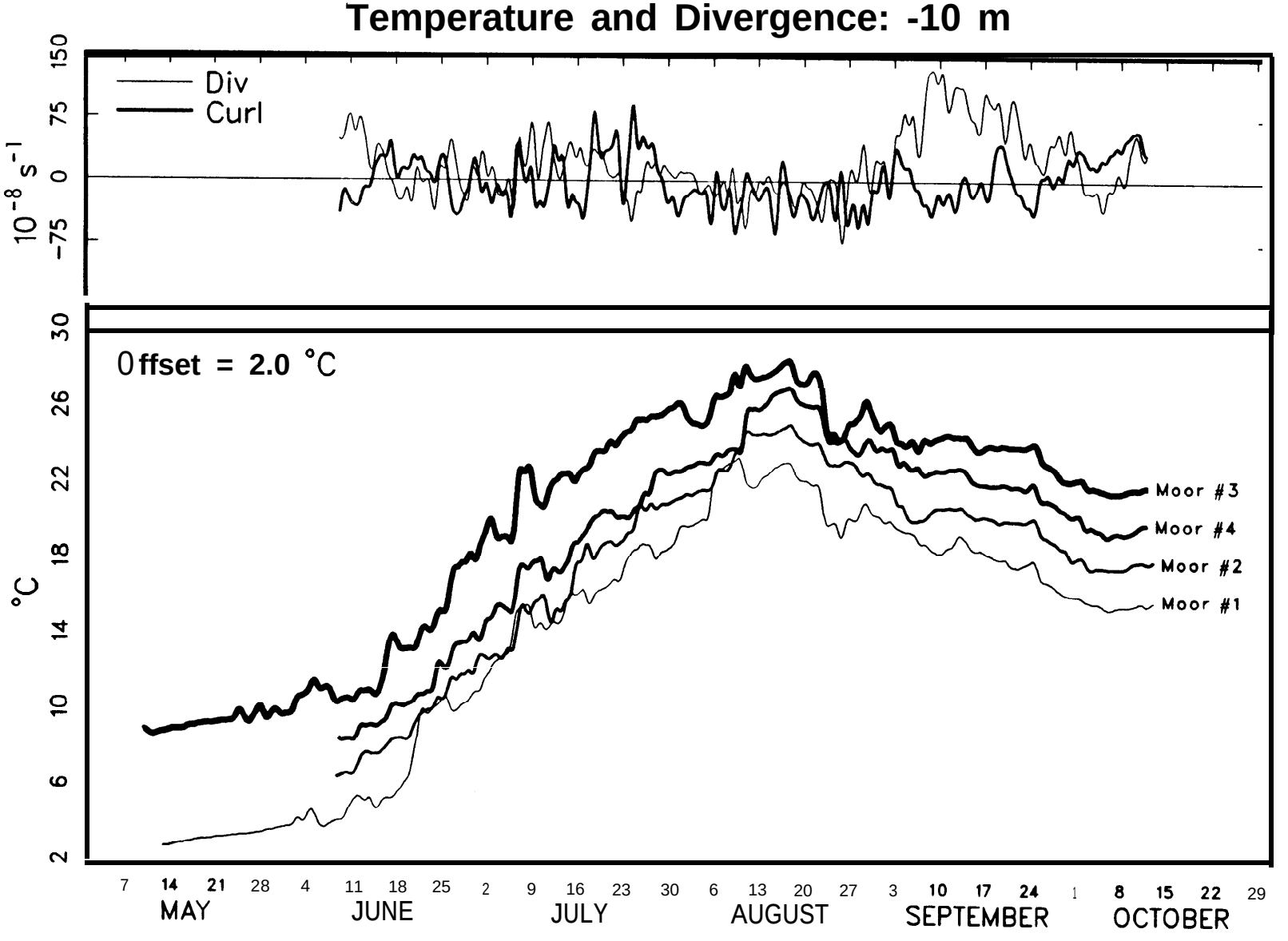
Temperature and Divergence: -10 m
Div
Curl
10^{-8} s^{-1}
150
75
0
-75
Offset = 2.0 °C
°C
30
26
22
18
14
10
6
2
Moor #3
Moor #4
Moor #2
Moor #1
7 14 21 28 4 11 18 25 2 9 16 23 30 6 13 20 27 3 10 17 24 1 8 15 22 29
MAY
JUNE
JULY
AUGUST
SEPTEMBER
OCTOBER
Lake Michigan 1984

Figure C.2

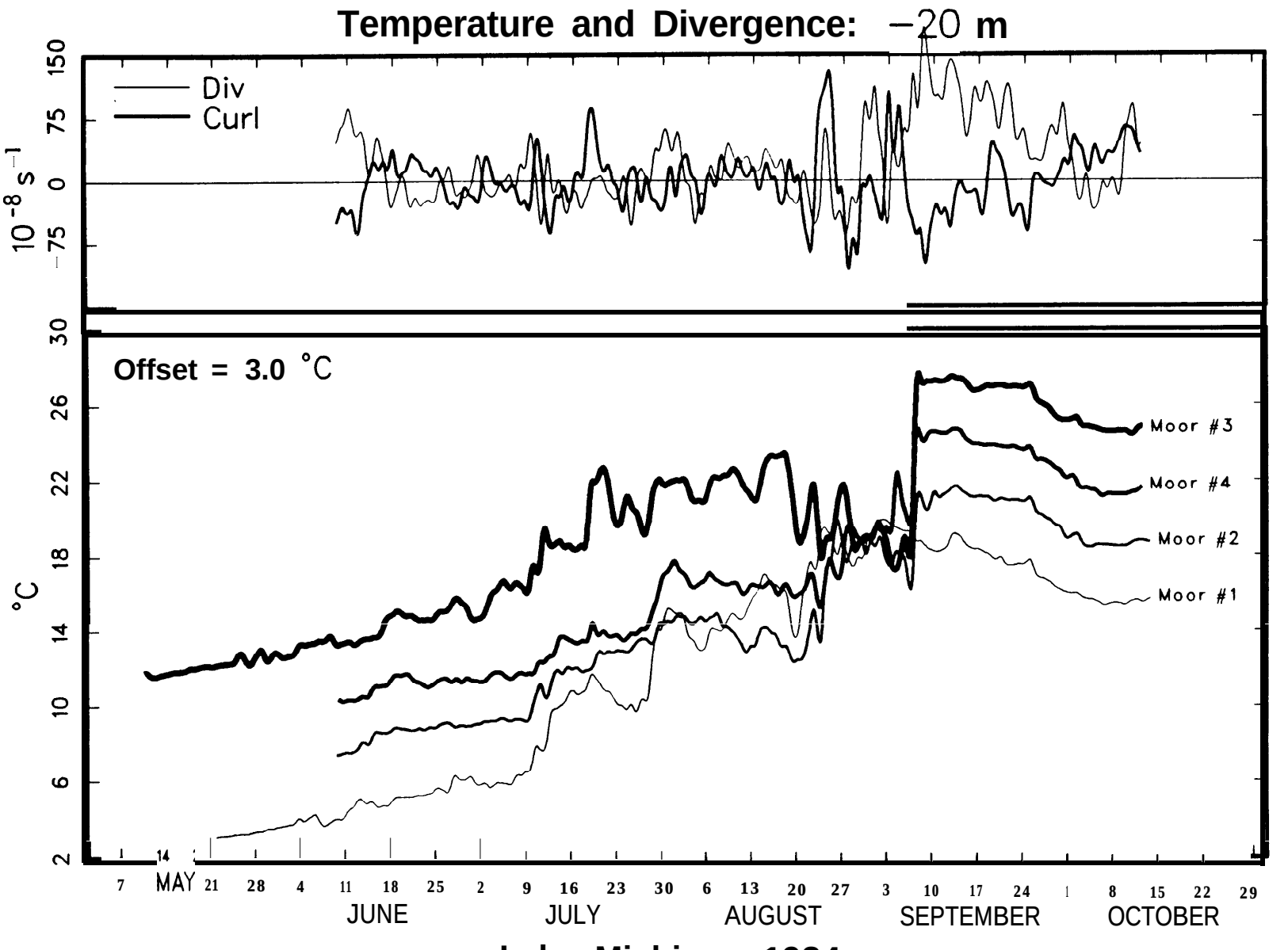
Temperature and Divergence: −20 m
Div
Curl
10^{-8} s^{-1}
150
75
0
−75
Offset = 3.0 °C
°C
30
26
22
18
14
10
6
2
Moor #3
Moor #4
Moor #2
Moor #1
7
14
MAY
21
28
4
11
18
25
2
9
16
23
30
6
13
20
27
3
10
17
24
1
8
15
22
29
JUNE
JULY
AUGUST
SEPTEMBER
OCTOBER
Lake Michigan 1984

Figure C.3

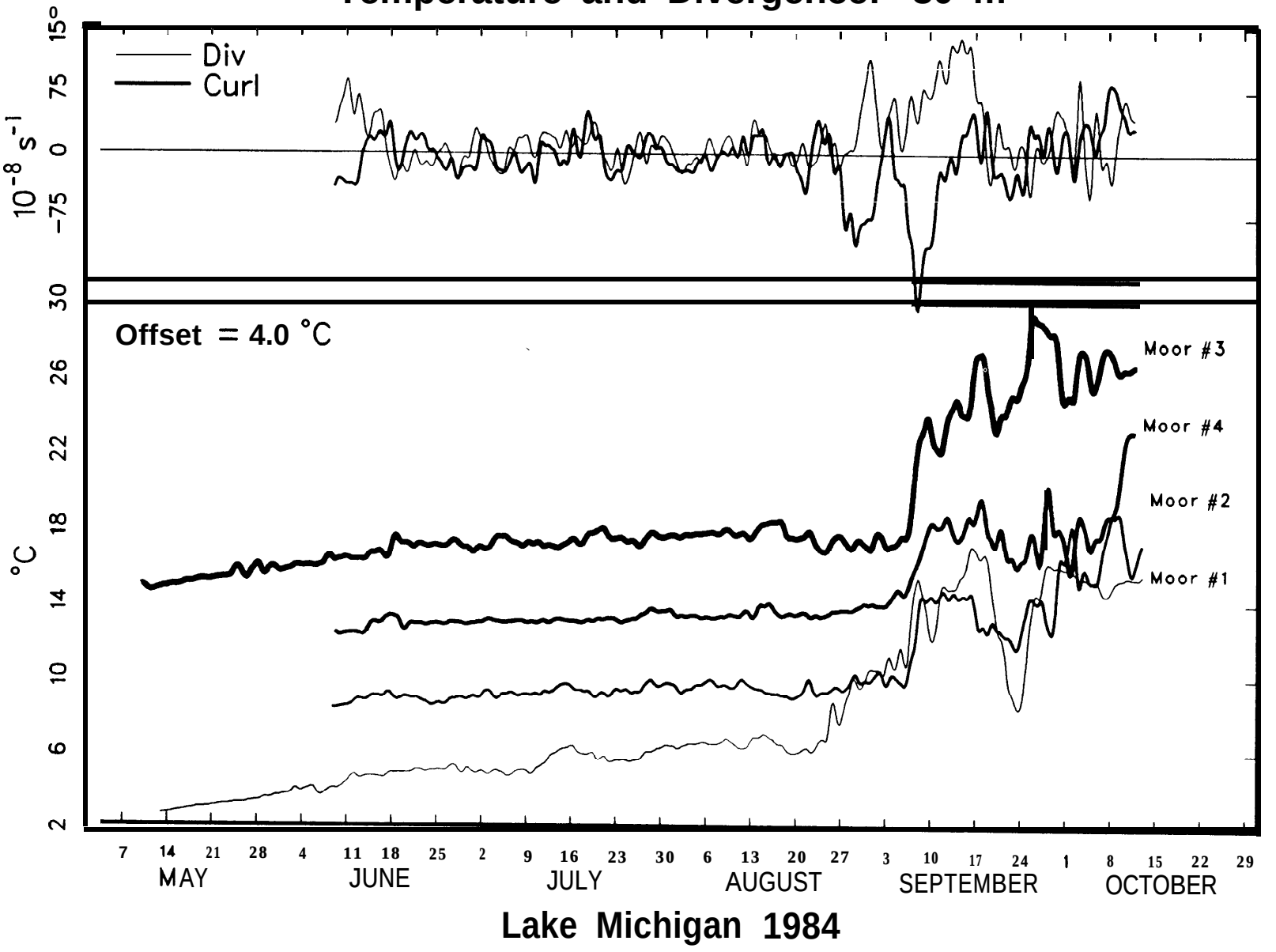

Lake Michigan 1984

Figure C.4

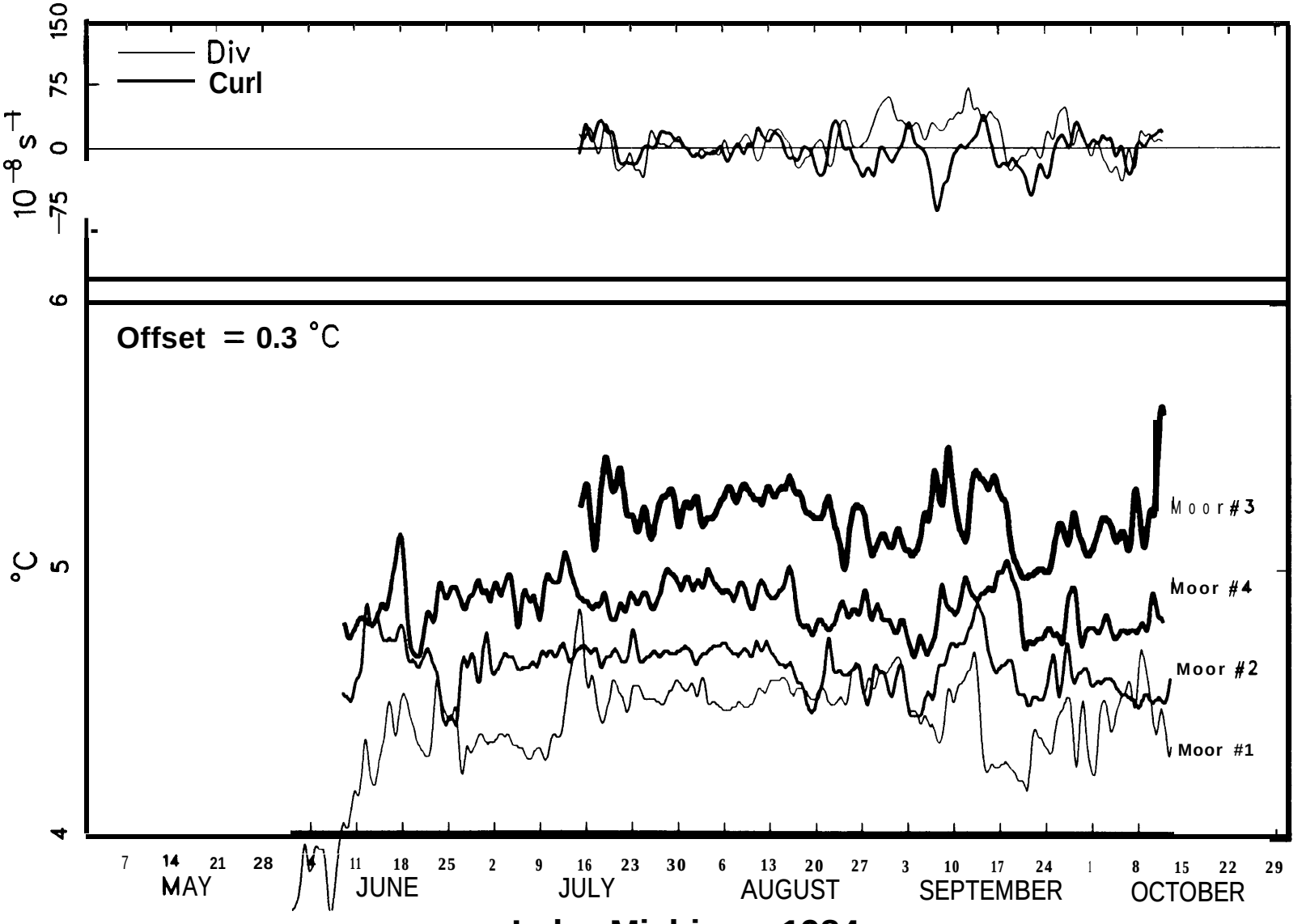

Lake Michigan 1984

Figure C.5

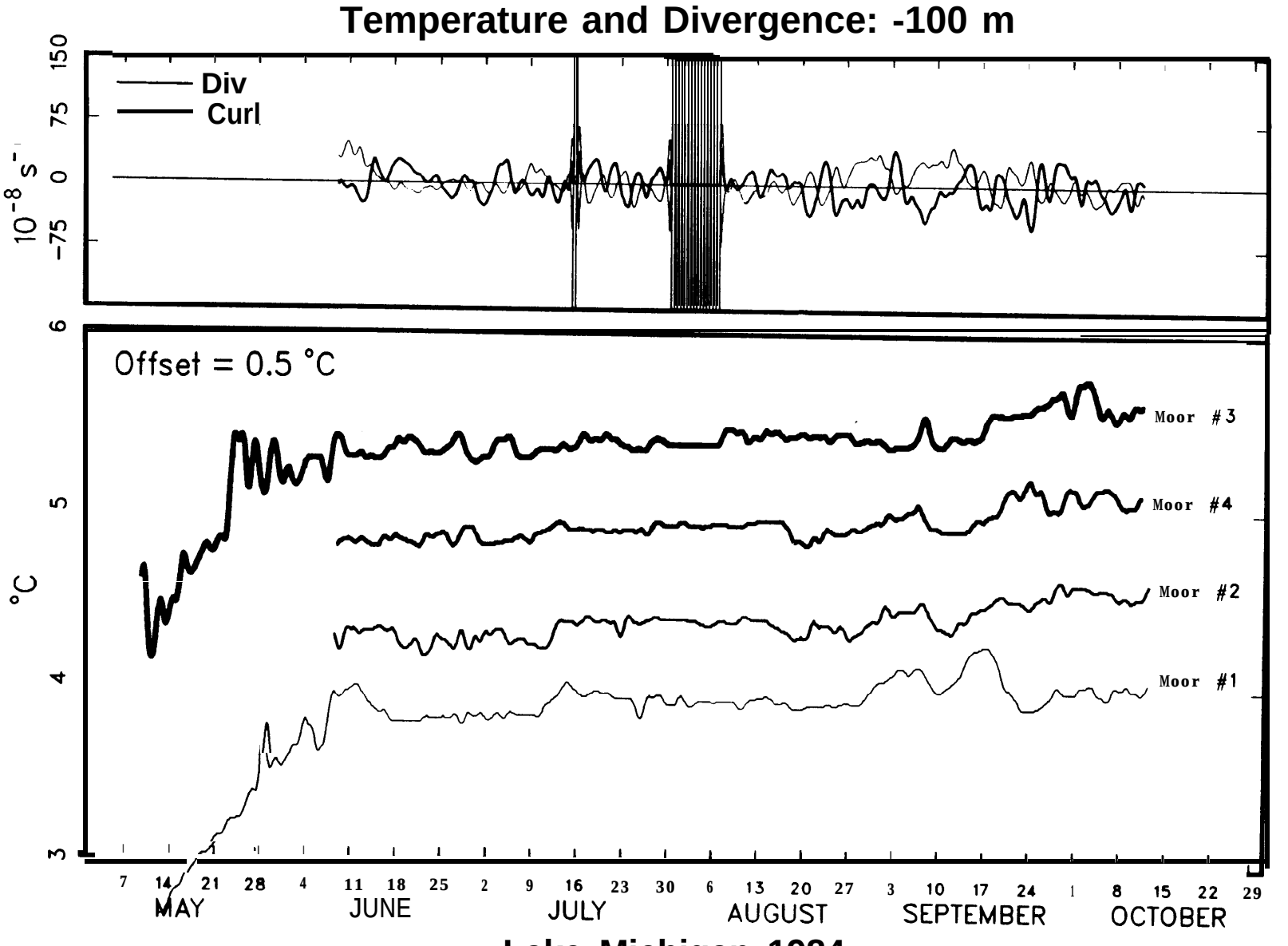

Lake Michigan 1984

Figure C.6

Appendix D: Separated Divergences

Figure 7. Plots of low-pass-filtered divergences computed across the three small triangles (see Figure 1), at the following depths:

Figure D.l--5 m
Figure D.2--10 m
Figure D.3--20 m
Figure D.4--30 m
Figure D.5--50 m
Figure D.6--100 m

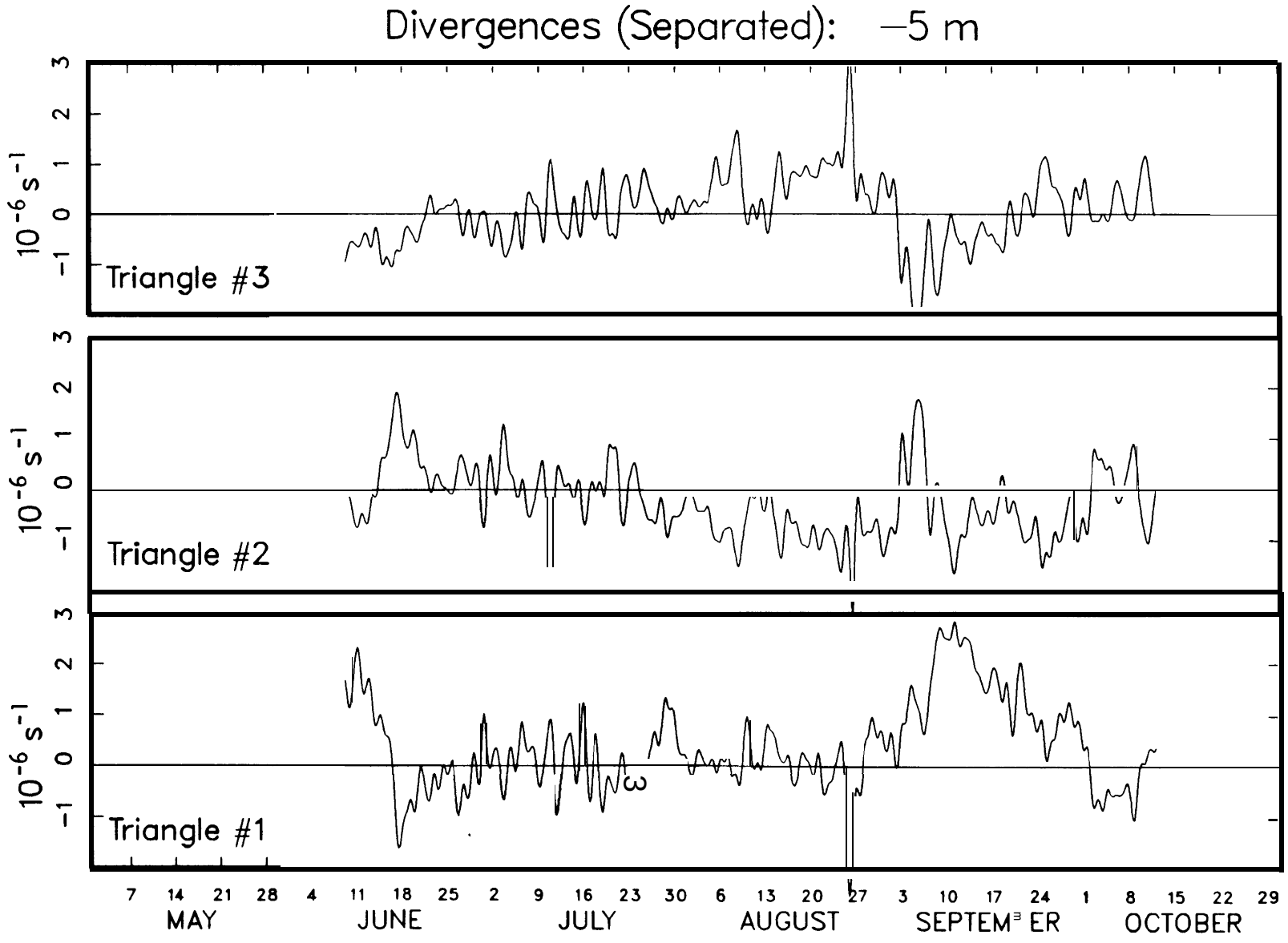
Divergences (Separated): −5 m
Triangle #3
Triangle #2
Triangle #1
10^{-6} s^{-1}
−1 0 1 2 3
7 14 21 28 4 11 18 25 2 9 16 23 30 6 13 20 27 3 10 17 24 1 8 15 22 29
MAY JUNE JULY AUGUST SEPTEMBER OCTOBER
Lake Michigan 1984

Figure D.1

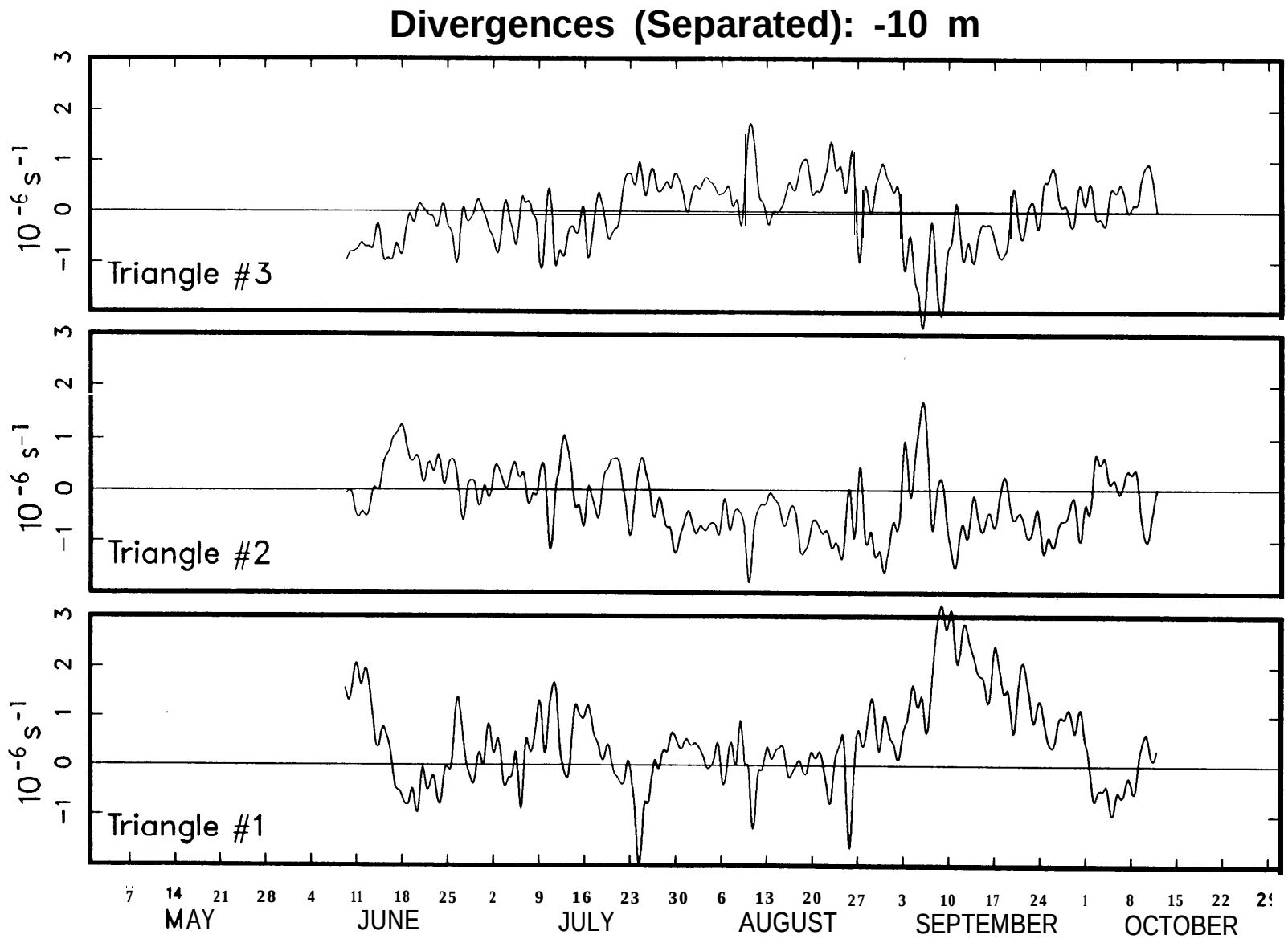
Divergences (Separated): -10 m
10^{-6} s^{-1}
3
2
1
0
-1
Triangle #3
Triangle #2
Triangle #1
7 14 21 28 4 11 18 25 2 9 16 23 30 6 13 20 27 3 10 17 24 1 8 15 22 29
MAY
JUNE
JULY
AUGUST
SEPTEMBER
OCTOBER
Lake Michigan 1984

Figure D.2

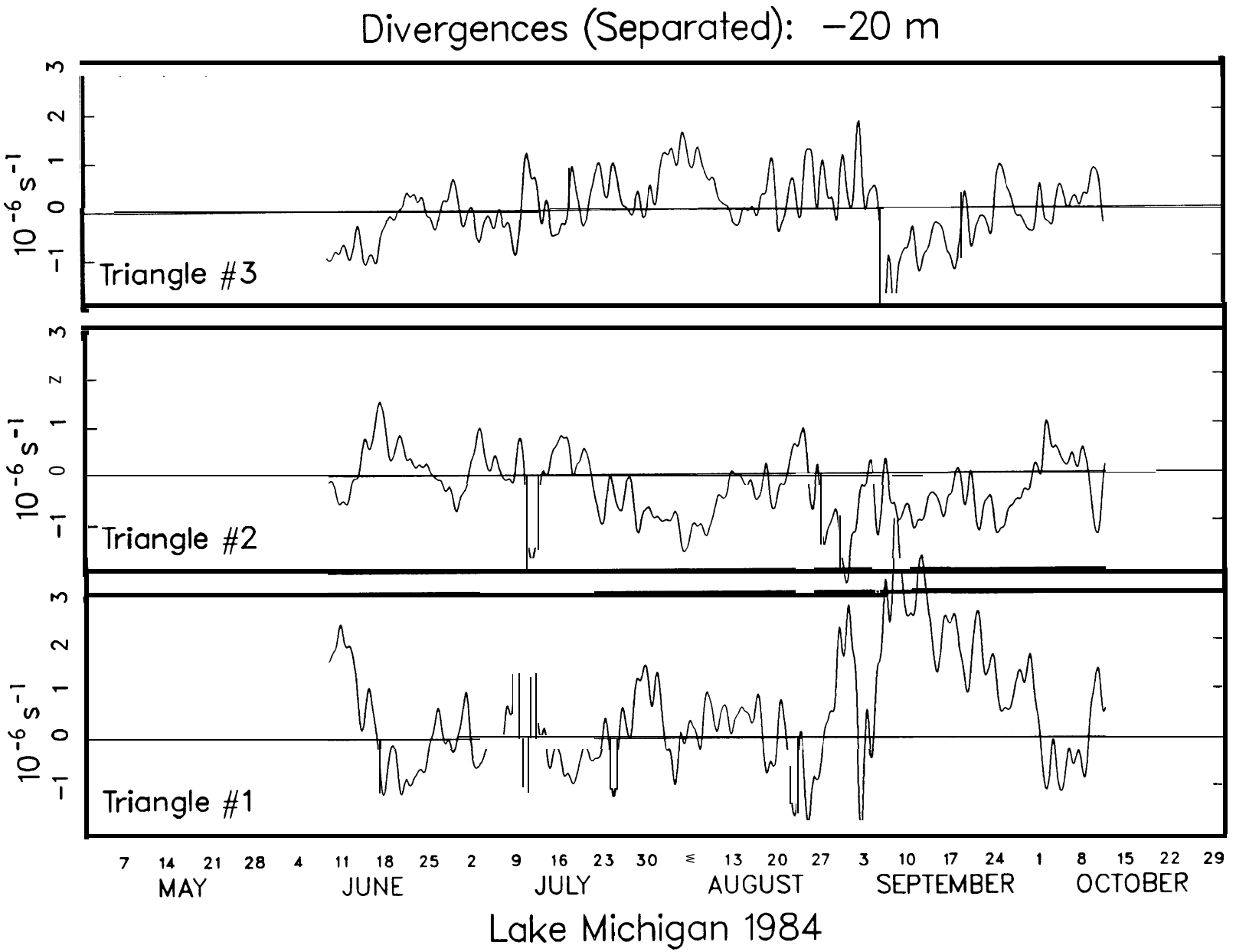
Divergences (Separated): −20 m
10^{-6} s^{-1}
3
2
1
0
−1
Triangle #3
Triangle #2
Triangle #1
7 14 21 28 4 11 18 25 2 9 16 23 30 13 20 27 3 10 17 24 1 8 15 22 29
MAY
JUNE
JULY
AUGUST
SEPTEMBER
OCTOBER
Lake Michigan 1984

Figure D.3

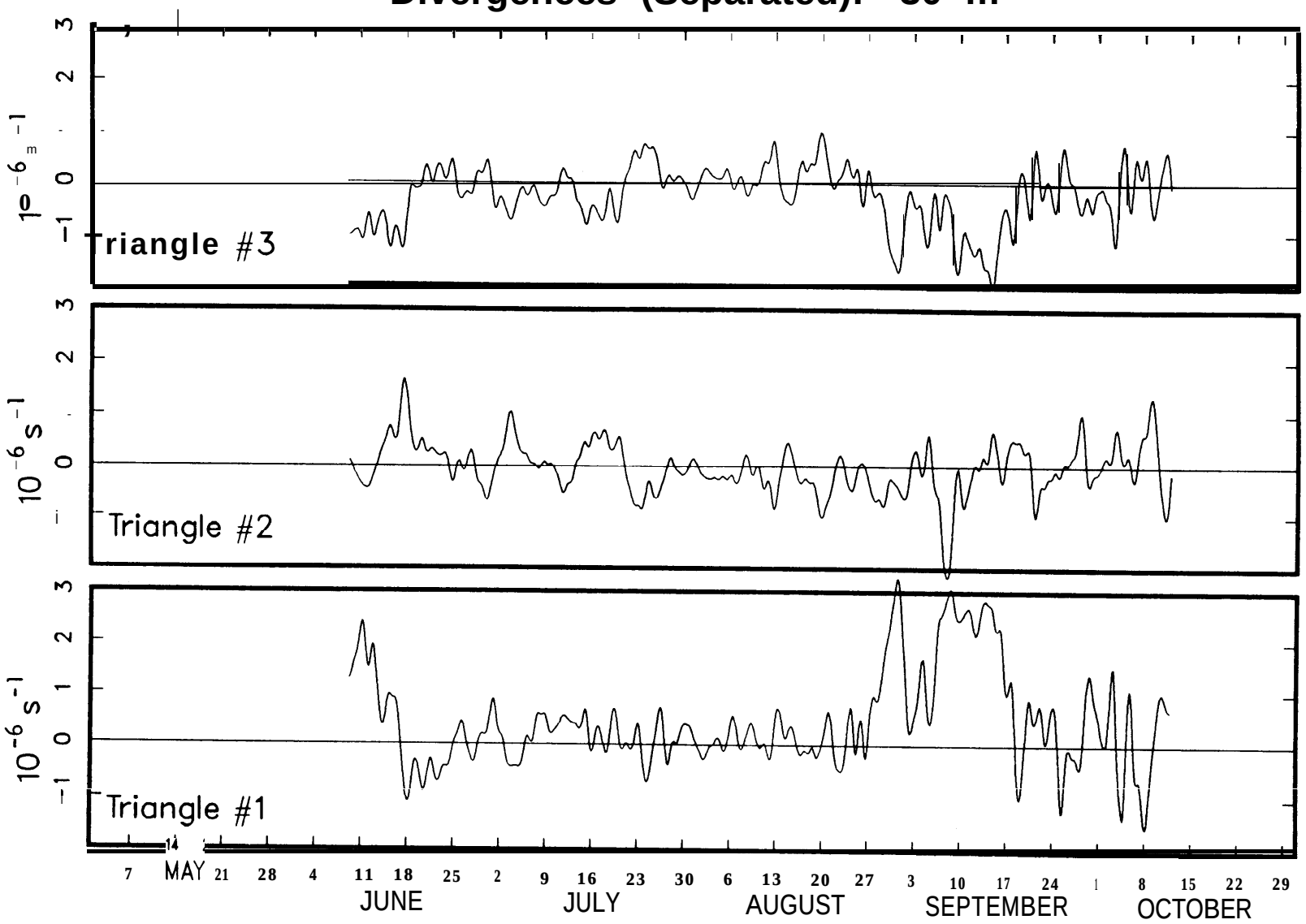
Divergences (Separated): -30 m
10^{-6} s^{-1}
Triangle #3
Triangle #2
Triangle #1
7 MAY 14 21 28 4 11 18 25 2 9 16 23 30 6 13 20 27 3 10 17 24 1 8 15 22 29
JUNE
JULY
AUGUST
SEPTEMBER
OCTOBER
Lake Michigan 1984

Figure D.4

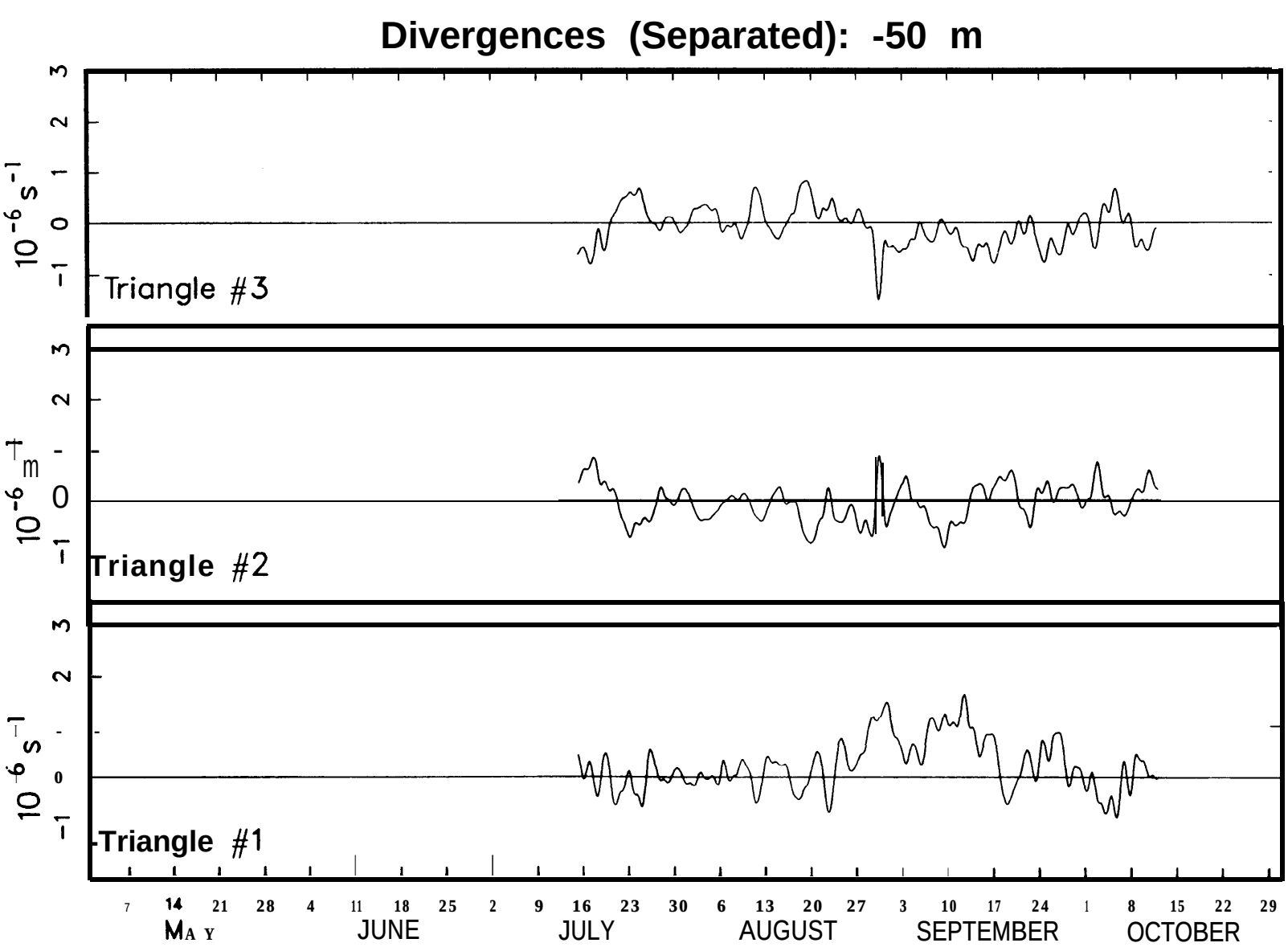
Divergences (Separated): -50 m
Triangle #3
Triangle #2
Triangle #1
10^-6 s^-1
10^-6 m^-1
7 14 21 28 4 11 18 25 2 9 16 23 30 6 13 20 27 3 10 17 24 1 8 15 22 29
MAY
JUNE
JULY
AUGUST
SEPTEMBER
OCTOBER
Lake Michigan 1984

Figure D. 5

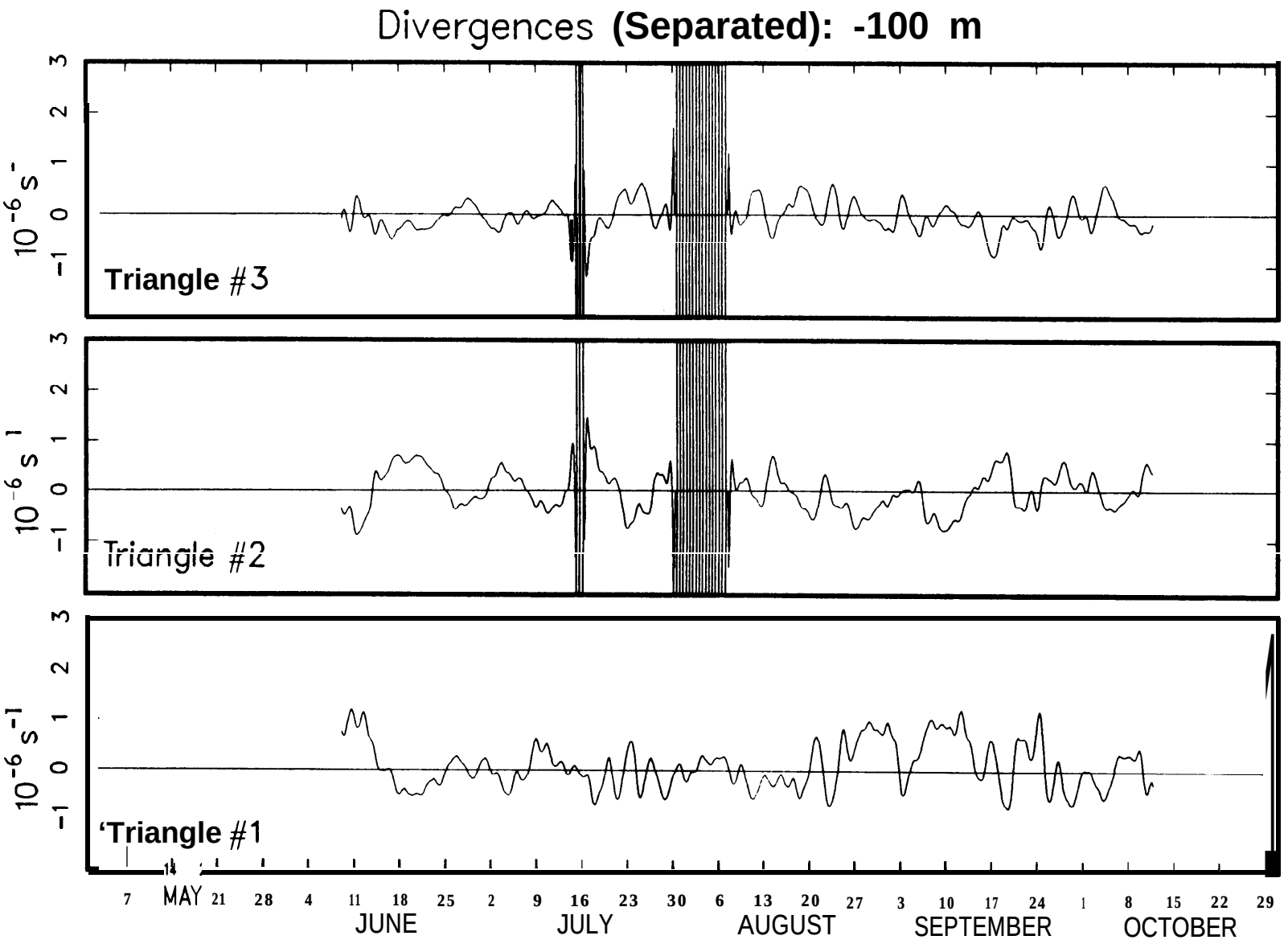
Divergences (Separated): -100 m
Triangle #3
Triangle #2
'Triangle #1
10⁻⁶ s⁻¹
7 MAY 21 28 4 11 18 25 2 9 16 23 30 6 13 20 27 3 10 17 24 1 8 15 22 29
JUNE
JULY
AUGUST
SEPTEMBER
OCTOBER
Lake Michigan 1984

Figure D.6

Appendix E: Raw vs. Filtered Data

Sample plots comparing the raw and the low-pass-filtered data during the months of August and September at 20 m depth. Shown are the u-component of current, v-component, and temperature for moorings 1 (Figures E.1-E.3) and 3 (Figures E.4-E.6).

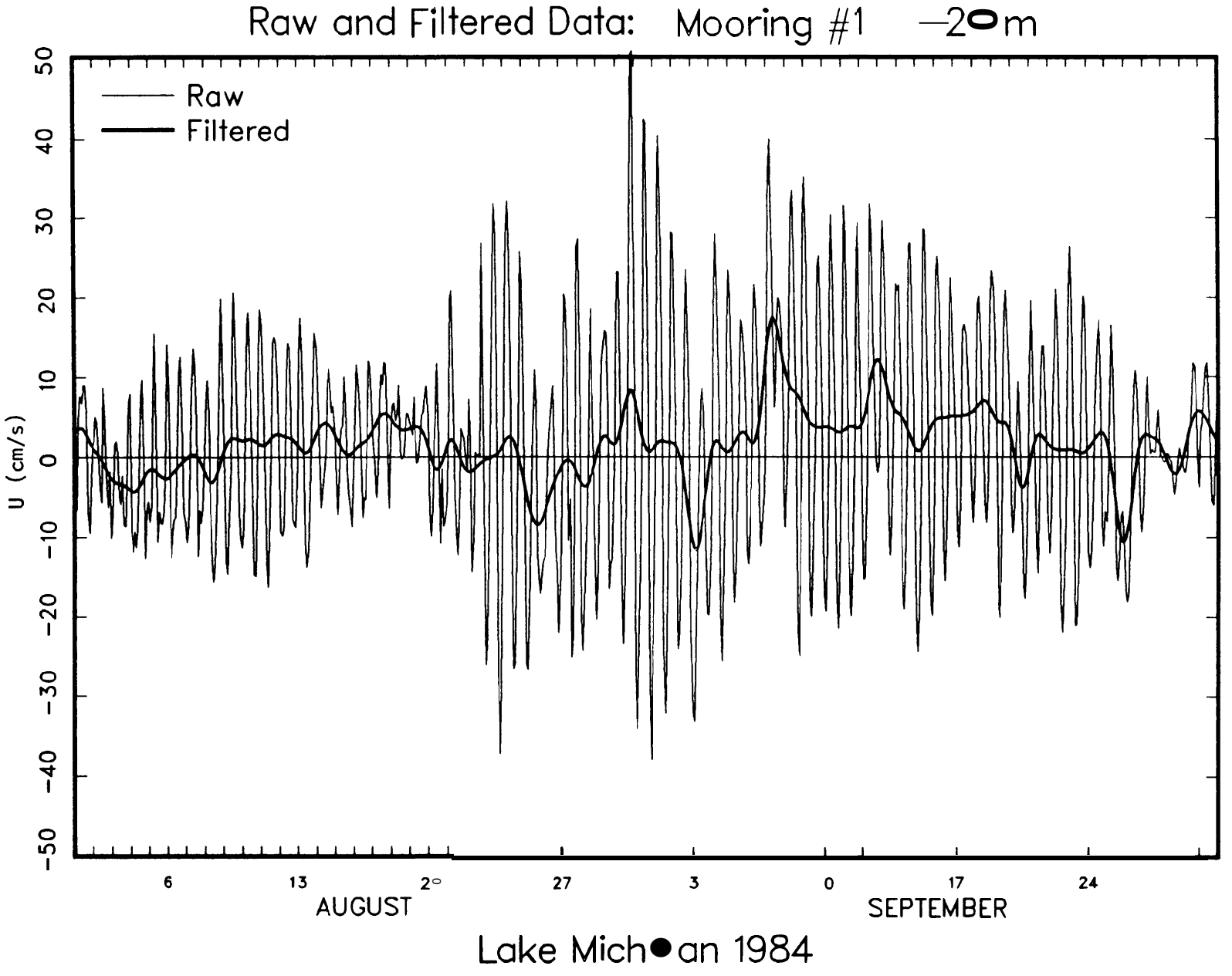
Raw and Filtered Data: Mooring #1 —20m
Raw
Filtered
U (cm/s)
50
40
30
20
10
0
-10
-20
-30
-40
-50
6
13
20
27
3
0
17
24
AUGUST
SEPTEMBER
Lake Michigan 1984

Figure E 1

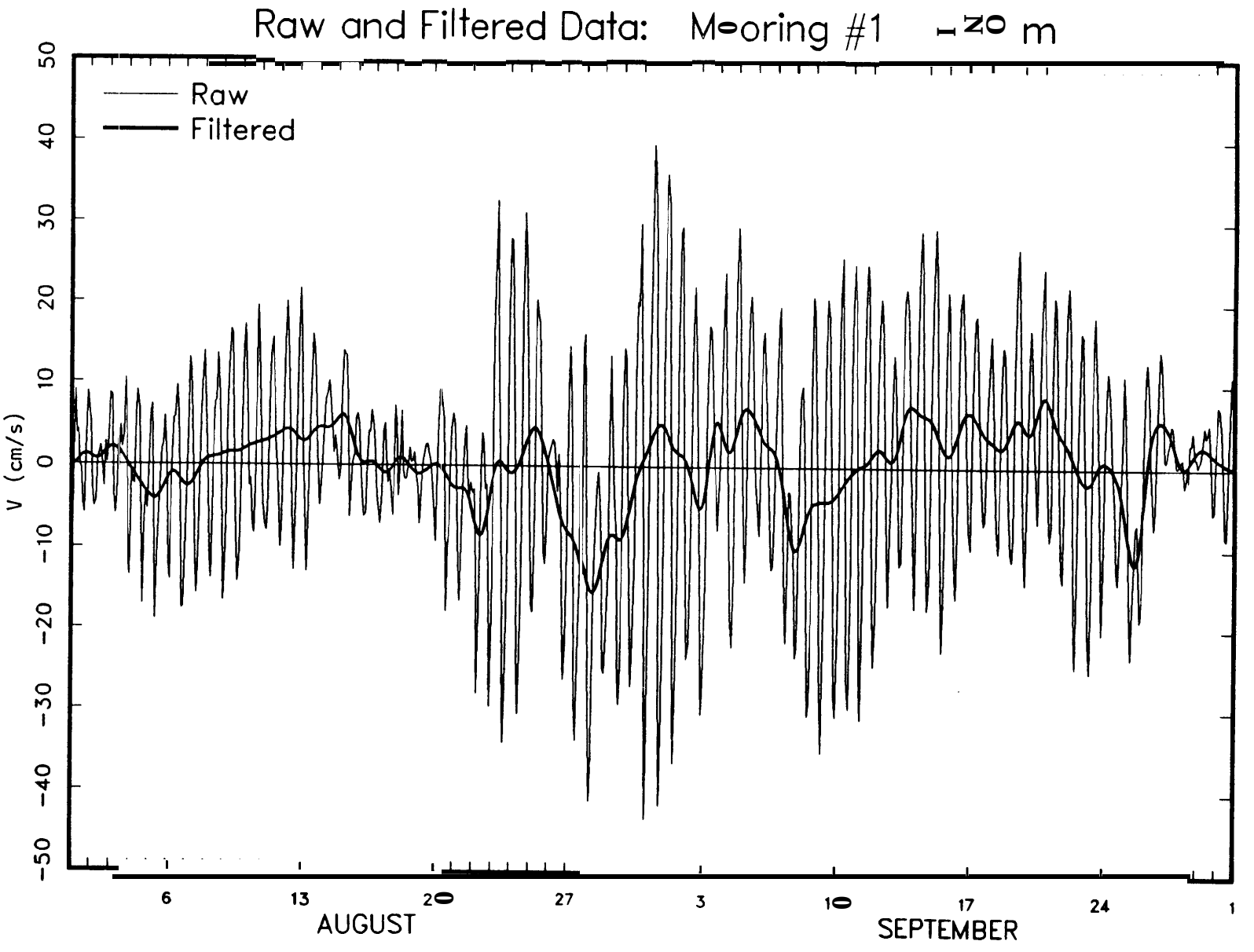

Lake Michigan 1984

Figure E 2

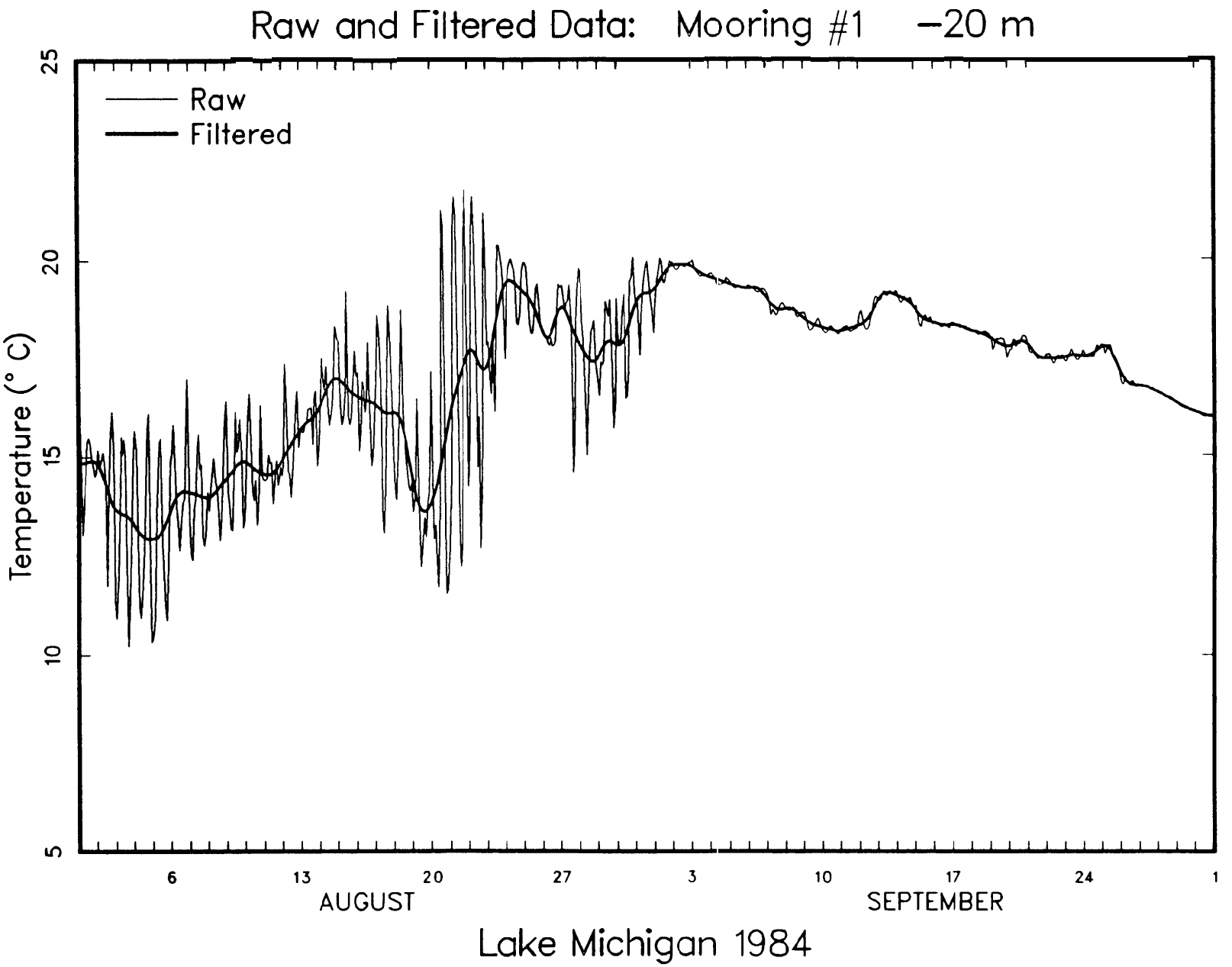
Raw and Filtered Data: Mooring #1 −20 m
Raw
Filtered
Temperature (° C)
25
20
15
10
5
6
13
20
27
3
10
17
24
1
AUGUST
SEPTEMBER
Lake Michigan 1984

Figure E.3

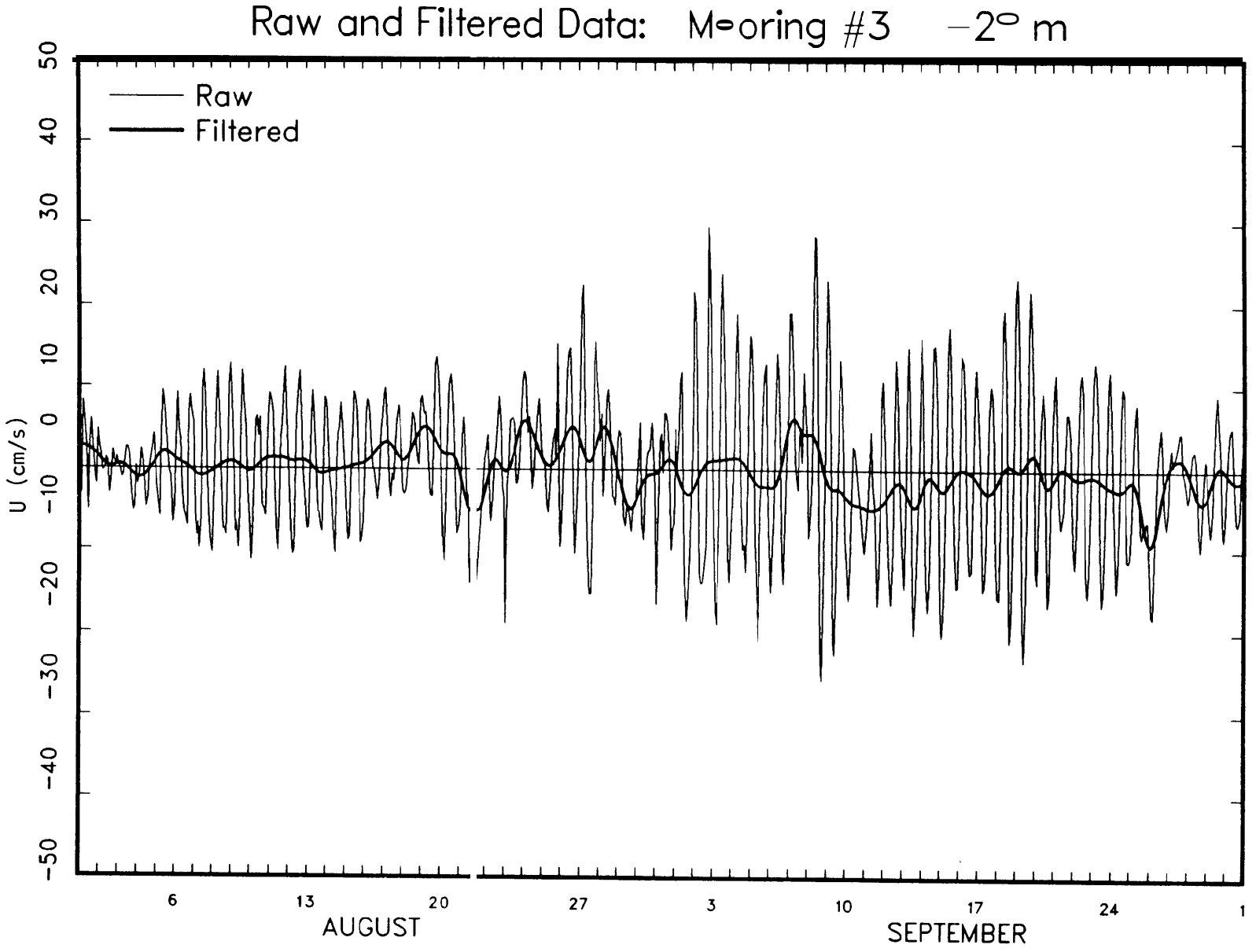

Lake Michigan 1984

Figure E.4

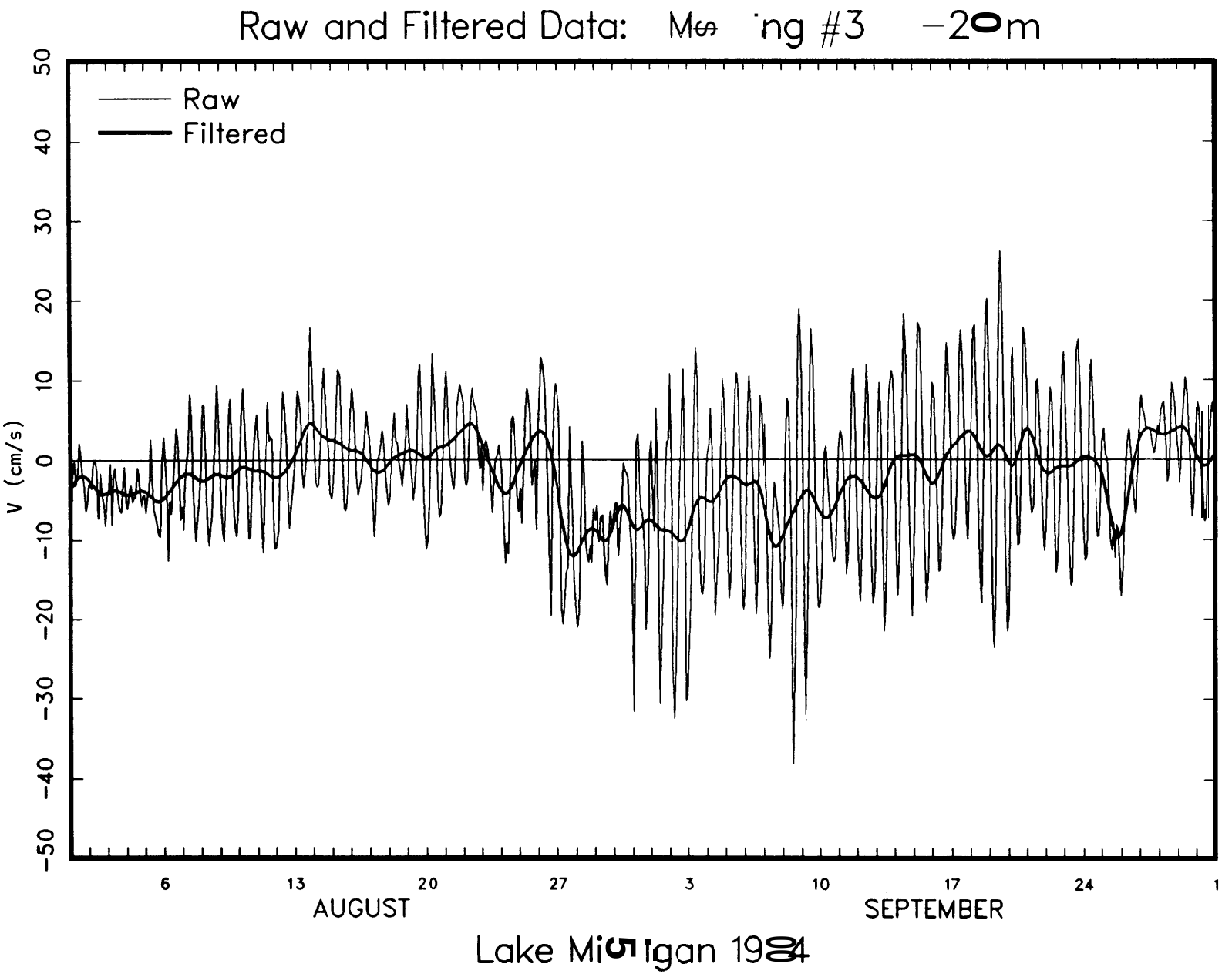
Raw and Filtered Data: M~~o~~ ing #3 −20m
Raw
Filtered
V (cm/s)
50
40
30
20
10
0
−10
−20
−30
−40
−50
6
13
20
27
3
10
17
24
1
AUGUST
SEPTEMBER
Lake Mi5 tgan 1984

Figure E.5

☆ U.S. GOVERNMENT PRINTING OFFICE: 1989—755-089

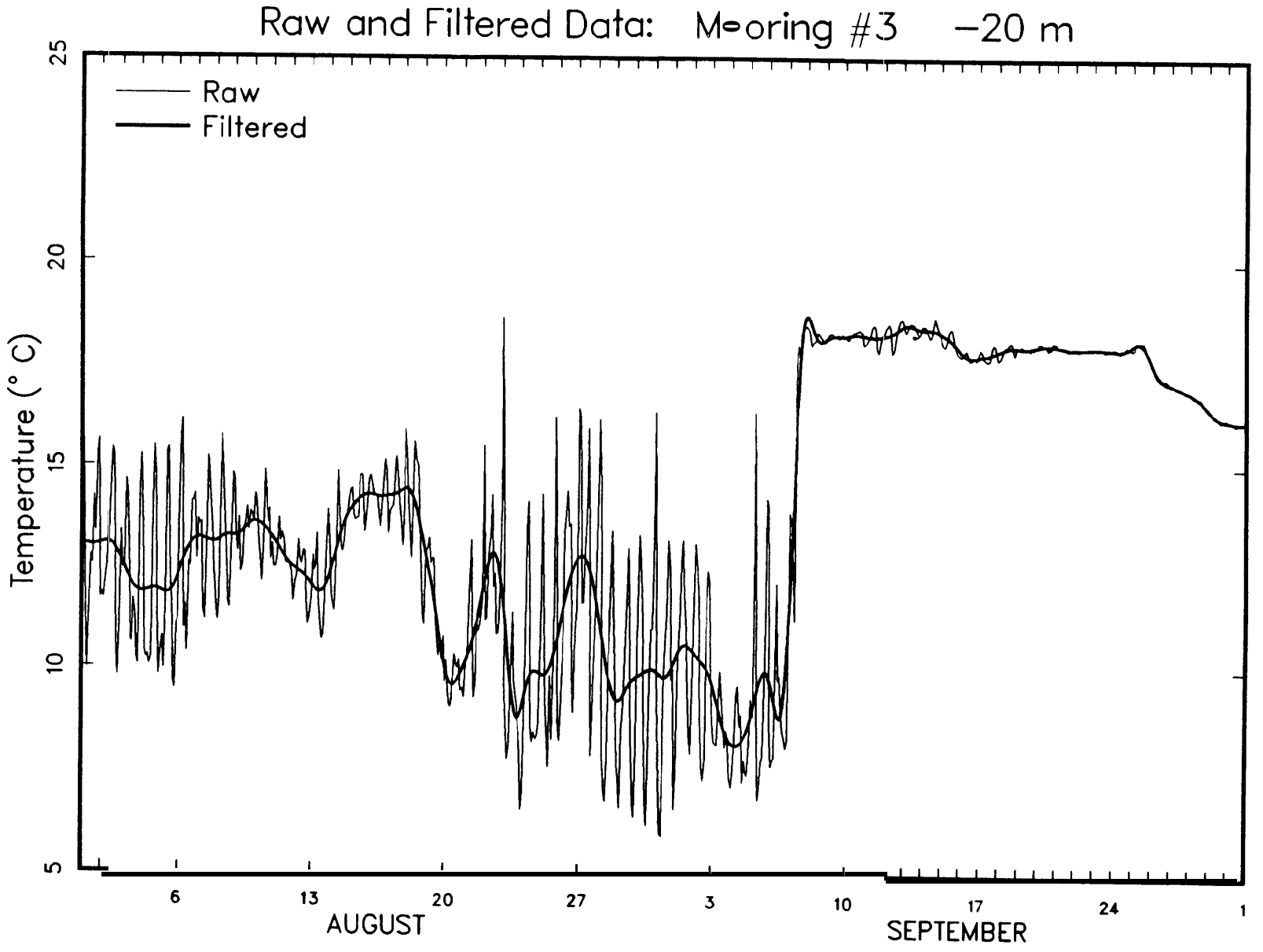

Figure E. 6